Unrevealing the Depositional Facies, and Diagenesis of Drug Formation in Zindapir Anticline, Sulaiman Province, Dera Ghazi Khan, Pakistan: Reservoir and Source Rock Characterization

By

Qurat Ul Ain

DEPARTMENT OF EARTH SCIENCES

QUAID-I-AZAM UNIVERSITY,

ISLAMABAD.

SESSION: 2021-2023

Unrevealing the Depositional Facies, and Diagenesis of Drug Formation in Zindapir Anticline, Sulaiman Province, Dera Ghazi Khan, Pakistan: Reservoir and Source Rock Characterization

A thesis submitted to Quaid-I-Azam University Islamabad in partial fulfillment of the requirement for the degree of Master of Philosophy in Geology.

By

Qurat Ul Ain

Supervised by

Dr. Abbas Ali Naseem

DEPARTMENT OF EARTH SCIENCES

QUAID-I-AZAM UNIVERSITY, ISLAMABAD.

SESSION: 2021-2023

Dedication

My Research Thesis is dedicated to, The only Sovereign of Heavens and Earth, Allah Almighty. This work is *also* devoted to the Holy Prophet Hazrat Muhammad (ﷺ), The Last Messenger of Allah Almighty. I also dedicate this work to my Mother, Yasmeen Munir, my Father, Munir Ahmad, and my respected teachers.

Acknowledgment

First and foremost all the praises and thanks to Allah Almighty for the courage and ability he gave me to work on this thesis project. If He did not want it for me I would never be able to complete my work. I would like to express my gratitude to my supervisor Dr. Abbas Ali Naseem, Associate Professor at the Department of Earth Sciences Quaid e Azam University, Islamabad, for believing in me and providing me with all the confidence. His sincerity and empathy inspired me. I am extremely grateful for what he has offered me. I would like to extend my heartful thanks to my parents and siblings and friends, especially Zubair Ahmed, for always being there for me on this journey and supporting me through thick and thin.

Qurat Ul Ain

Abstract

In this research work Eocene's Drug Formation of 583m, measured in the Zindapir Anticline section is systematically sampled from each bed. Detailed petrographic analysis and microfacies study is conducted on the collected samples, furthermore, porosity, permeability, and plug analysis were also performed. The objectives were to specify the microfacies and their depositional environments and diagenetic changes as well as reservoir and source rock characterization. On the base of microfacies analysis Drug Formation is classified into twelve different facies which disclosed that the formation is deposited in the inner-shelf environment embracing tidal (MF1), lagoonal (MF2-MF5), back-reef (MF6-MF9) and fore-reef (MF10-MF12). Diagenetic alteration is studied from early to late stages. In eodiagenesis, micritization and bioturbation took place in significantly shallow marine environments and dissolution in meteoric environments. During mesodiagenesis cementation of blocky calcite, compaction, and dolomitization along the fluid path occur. Fracturing is caused during telodiagenesis. TOC of studied samples shows Drug Formation is fair to poor source rock and has an immature production index. The plug analysis of selected facies shows that the depositional texture of Drug Formation is impervious and of poor reservoir quality.

Table of Contents

List of Figures

CHAPTER 2

CHAPTER 3

CHAPTER 4

CHAPTER 5

CHAPTER 6

List of Tables

CHAPTER 2

CHAPTER 6

CHAPTER 1

Introduction

1.1 General Introduction

Typically, sedimentary carbonate rocks result from deposition in neritic habitats such as marine environments. On average, 32.2% of sedimentary rocks are comprised of calcium carbonates (Chilingar et al., 2011). The formation of carbonate rocks involves mechanical, organic, chemical, and inorganic processes. The production of carbonates is influenced by temperature, water salinity, and light penetration. Factors like geological settings, sea level changes, climatic stability, turbidity, substrate type, nutrient flux, and wave/current regimes highly impact carbonate production. Carbonate includes more than 50% carbonate minerals (such as calcite and dolomite). Limestone is a rock with a carbonate content greater than 50%, with calcite or aragonite making up more than half of the composition. The rock is called dolostone if most of the carbonate material is dolomite (Selley, 2005). Limestone ($CaCO_3$) and dolomite ($CaMg(CO_3)_2$) are major carbonate rocks. Carbonate rocks are mainly composed of three components called allochemicals compounds, matrix, and cement.

Microfacies analysis is utilized to examine the taxonomy, taphonomy, paleoecology of major and minor events, and for paleoenvironmental reconstructions in carbonates. Lithofacies of a stratum helps interpret the depositional settings and the development of sequence stratigraphy, diagenetic history, and porosity and permeability evolution (Carozzi, 1988; Ahmad et al., 2020). Microfacies analysis assists in outcrop and fossil interpretations providing sufficient information on paleoenvironment and sea level change and is crucial for creating a foundation for sequence stratigraphy for carbonates and clastics (Serra-Kiel et al., 2003; Ahmad et al., 2020). A considerable amount of knowledge regarding paleoenvironments and sea-level fluctuations may be obtained by microfacies analysis of an outcrop and its fossil interpretation. Establishing a sequence stratigraphic structure relies on it (Serra-Kiel et al. 2003).

Carbonate rocks contain over 50% of the oil and gas reserves of the whole world, with 40% of the reservoirs located mainly in Asia (Schlumberger, 2007). Reservoir characterization is a core part of the activities involved in assessing and mitigating formation damage. It provides information about the three-dimensional distribution and manifestation of the

reservoir heterogeneity and petrophysical properties (Lucia et al., 2003). When formation damage or stimulation occurs, reservoir properties change over time. A crucial aspect of reservoir characterization is learning and precisely mapping the features and heterogeneity of the reservoir. Conventional approaches frequently fall short of correctly allocating the reservoir or estimating its complex features, especially in carbonate reservoirs, which provide substantial challenges in petroleum exploration. The heterogeneous characteristics of a carbonate reservoir pose severe challenges and might cause a failure in reservoir prediction (Moqbel, 2011). Alongside the conventional methods, several researchers presented additional techniques that improve the estimation of permeability using log data and core data with the help of data classification (Hearn et al. 1984; Perez et al. 2005; Moqbel and Wang 2011; Ferraretti et al. 2012). Hydraulic units (HU) and electrofacies (EFs) have gone mainstream recently for differentiating complicated heterogeneous reservoir issues by dividing the reservoir interim homogenously based on comparable petrophysical parameters (Serra and Abbott 1980; Deghirmandjian 2001; Skalinski and Kenter 2013; Rahim et al. 2013; Mode et al. 2014; Plastino et al. 2017; Yasin, 2019).

Following the deposition, lithification of sediments took place which is followed by the changes like compaction, cementation, dissolution, mineral replacement, recrystallization, or dolomitization during the burial (Lapponi et al., 2014). Pressure and temperature variations have a physical, chemical, and biological impact on strata. This process of diagenesis results in the cementation, development of secondary porosity, and replacement of previous elements. It is independent of any depositional environment. Such diagenetic alterations remove the original impressions and textures (Smith and Simo, 1997; Nichols, 2009). The primary process of diagenesis is lithification, which hardens the soft deposited sediments turning them into rock. Grabau (1924) defined lithification which includes processes like dehydration, crystallization, recrystallization, compaction, and cementation. Geochemical factors in diagenesis also explained by Grabau (1924) include low temperature & metasomatism, hydration & dehydration, ion exchange, and polymerization & depolymerization.

1.2 Location of the Area

The study area is located on the Eastern limb of the Zindapir anticline located in Dera Ghazi Khan, a city in the southwestern part of Punjab province, Pakistan. It is situated in close proximity to the Sulaiman Range, which is a prominent mountain range in the region. The Sulaiman Range is known for its complex geological history and diverse geological formations.

The 130 km long Zindapir anticline, which is north-south orientated, is located on the mountain front of the SFTB.

1.3 Climate of the Area

The study area experiences significant variations in temperature throughout the year, with hot summers and relatively cooler winters. During the summer season, temperatures can soar as high as 115 °F (46 °C), creating extremely hot and arid conditions. These high temperatures are characteristic of the region's desert-like climate, with limited vegetation and intense solar radiation. In contrast, the winter season brings comparatively milder temperatures, with lows dropping to around 40 °F (4 °C).

1.4 Aims and Objectives

The research project intends to investigate the Drug Formation within the Zindapir Anticline located in the Sulaiman Province, with a focus on microfacies analysis, reservoir, and source rock characterization. Understanding the formation's sedimentological, petrological, and geochemical features is key to determining its reservoir potential and assessing the properties of its hydrocarbon source rock.

a. The study's main objective is the detailed analyzation the Drug Formation's microfacies. This entails a methodical description and interpretation of microfacies. A microfacies analysis aims to locate and describe the biotic elements, sedimentary textures, and depositional settings present in the formation. The study aims to distinguish between several microfacies types, such as grain-supported, mud-supported, or wackestone-packstone-grainstone-dominated facies, by examining thin sections and petrographic samples. This goal will shed light on the diagenetic processes, paleoenvironmental settings, and depositional settings that impacted the sedimentary structure of the formation.
b. Microfacies will characterize their relative environment forming a depositional model giving insights into the paleoenvironment in which microfacies are deposited.
c. The third aim is to evaluate the reservoir characterization of Drug Formation, which tells the capacity of accumulation of hydrocarbons by the formation. Analyzing important reservoir variables like porosity, and permeability is required for this. The study's goal is to identify the formation's reservoir quality, heterogeneity, and fluid flow characteristics through the air porosity, permeability, quality index, and reservoir flow zone index.

d. Lastly, this study aims to do source rock evaluation of Drug Formation. This entails looking at the formation's geochemical makeup, thermal maturity, and organic matter content. The study intends to evaluate the source rock potential, organic richness, and thermal maturity levels of the formation by analyzing rock samples and performing geochemical tests, such as organic petrography, Rock-Eval pyrolysis.

CHAPTER 2

Regional Tectonics and Stratigraphy

2.1 Tectonics of Pakistan

The Indian Plate collided with the Eurasian Plate about 50 and 56 Ma ago, eventually closing the Tethys Ocean, caused the Himalayan orogeny (Green et al., 2008; Ding et al., 2016; Qasim et al., 2018). Both plates being dense continental plates could never be subducted underneath any of the other so a Himalayan relief was produced by rise of the less density rocks. The Indus Tsangpo Suture Zone, which separates the Indian and Eurasian plate (Tahirkheli, 1979; Jin et al., 1996).

Himalayan collision zone contains a series of fold-thrust belts on the eastern side while it constitutes left-lateral strike-slip faults, is Chaman Fault on the westernmost region with a length of about 900km, also marks Indian-Eurasian collision in the westward region (Abdel-Gawad, 1971; Farah et al.,1984; Qayyum et al., 1996; Stein et al., 2002). Pakistan is tectonically divided by these fold-thrust belts creating mountain ranges that stretch from the northeast Salt Range to the Sulaiman and Kirthar Ranges in the southwest, next to the plains of Indian Plate. Arabian Plate subducts under Indian Plate this is the point where these strike-slip faults joined the Makran Convergence zone and folded in the eastwest side (Quittmeyer & Jacob, 1979; Lawrence et al., 1981; Vernant et al., 2004); connecting it with the Indian and Eurasian Plate convergence in the north.

The Sulaiman Ranges run along the northwestern boundary of the Indian Plate and a remarkable tectonic phenomenon (Ullah et al., 2020). The western boundary of the Indian Plate makes an angle that is significantly oblique with the relative motion of Indian and Eurasian Plates in the area. It follows that a substantial proportion of left-lateral shearing. The convergent boundaries of Indian and Eurasian Plates brought the variation in elevation and also caused the shortening. The chain of strike-slip faults, Chaman Faults, induced also fold and thrust faults in the southeast side (Szeliga et al., 2012) due to a broad transpressional zone that produces occasional seismicity along northeastern to western boundary (Quittmeyer & Jacob, 1997; Prevot et al., 1980). Eastern side of Sulaiman range comprises of a string of left-lateral strike-slip faults, like Kingri fault, resulting from the north-south convergence of the Indian and Afghan Block (Rowlands, 1978; Jadoon et al., 1994).

2.2 Sulaiman Basin

At the westernmost edge of the Pakistani Himalayas is an important tectonic structure known as the Suleiman Fold and Thrust Belt (SFTB). The SFTB has a lobed geometry resulting from the convergence of the Indian and Eurasian plates (Jadoon and Khurshid, 1996; Reynolds et al., 2015). Sulaiman fold and thrust belt are comprised of a number of subsurface folds and faults (Kazmi and Rana, 1982; Jadoon and Zaib, 2018). SFTB is the closest structure to the collision zone proved by a number of anticlinal features in the vicinity. Structural variation in Sulaiman ranges runs from northwest-southeast to eastwest to northeast-southwest or north-south in all eastern, central, and western parts but there is an absence of thrust faults on the mountain front (Reynolds et al., 2015). The 130 km long Zindapir anticline, which is north-south orientated, is located on the mountain front of the SFTB. Indian and Eurasian collision divided the plates into several fragments. In the East of Zindapir there lies the Sulaiman fold and thrust belt and Sulaiman depression, while west of it is the Barthi syncline. Zindapir anticline is a consequence of the long-hidden subsurface sinistral fault and is also known as Koh-Safed elevation. It is the biggest and most elevated structure. Nature of Zindapir anticline results in occasional sinistral motions (Bannert et al., 1995).

In central Pakistan at northwest edge, Mesozoic to Paleogene succession is extensively exposed. These strata were formed after the Tethy's closure (Cheema et al 1977, warwick et al 1998). The Dunghan Formation of Paleocene to Eocene age, the Shaheed Ghat Formation of Early Eocene, Drug and Baska Formation, and the Kirthar Formation (Middle Eocene to Late Eocene) make up the Paleogene Sequence of the Suleiman Ranges, which sits above the strata of the Mesozoic era (Warraich et al., 2000).

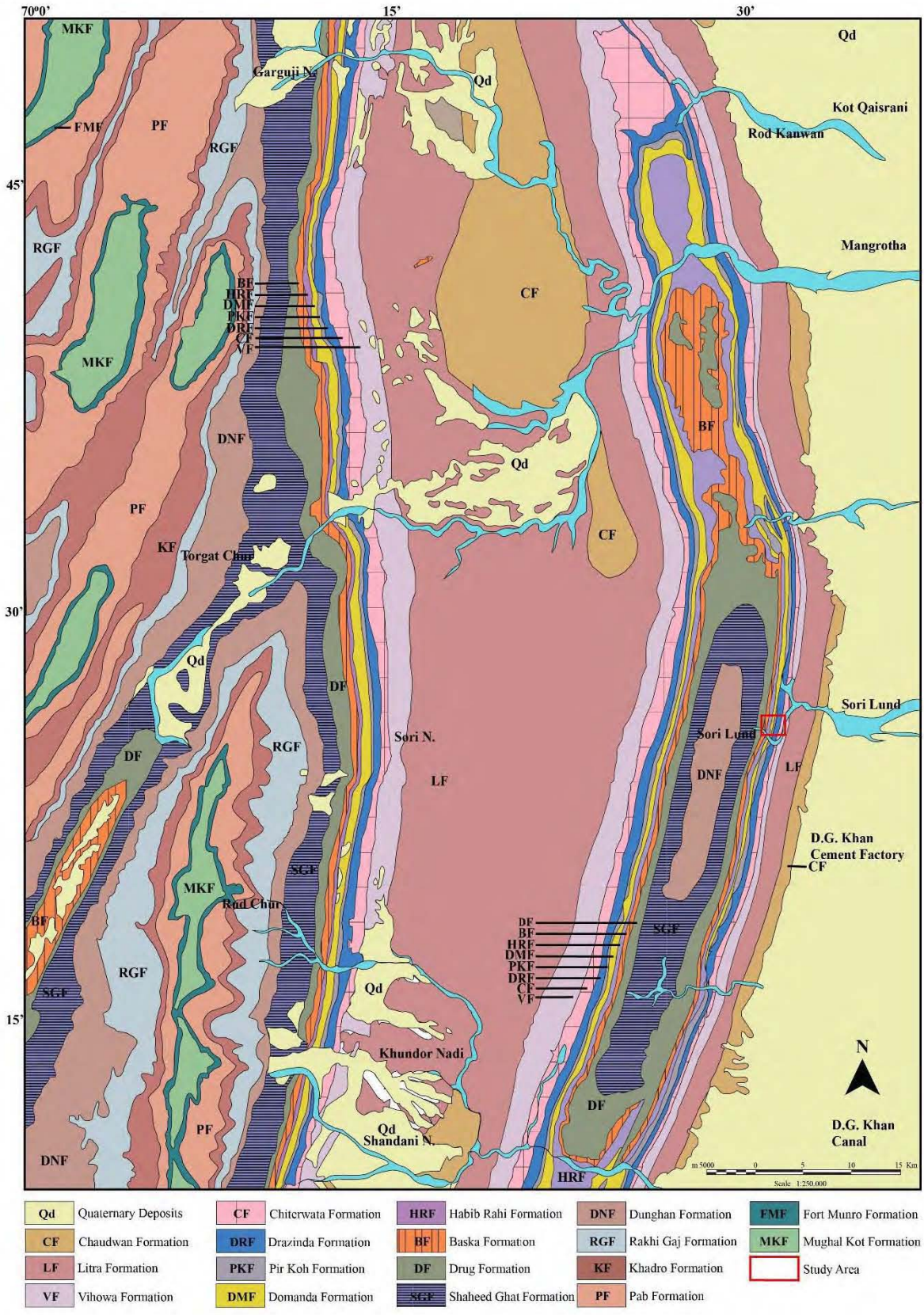

Figure 2.1: Zindapir Anticline Map of Dera Ghazi Khan (Hassan et al., 2002).

2.3 Stratigraphy of Study Area

Axial plane belt divides Indus basin (Gondwana land) and Balochistan Basin (part of Lurasia). The Indus basin, which is additionally divided into the Kohat (upper) and Potwar, middle Sulaiman, and lower Kirthar basins, is where the central and eastern regions of Pakistan are located. The Sulaiman Basin is the biggest basin, covering 170,000 km^2. The noteworthy features of Sulaiman basin are SFTB, Sulaiman foredeep zone and southern Punjab monocline. The Indus basin is divided solely and primarily on the base of diverse lithostratigraphic characteristics, for instance, the Eocene strata from Sulaiman basin vary from the Eocene strata of Kirthar basin. Sulaiman basin is composed of sedimentary rocks from Jurassic to the recent age. Eocene strata in the Sulaiman basin consist of Ghazij group and Kirthar Formation (Malkani, 2010; Malkani and Mahmood, 2017). (Table 2.1)

Table 2.1: Eocene strata in Zindapir Anticline.

Kirthar Formation	Members	Drazinda Formation
		Pirkoh Formation
		Domanda Formation
		Habib Rahi Formation
Ghazij Formation	Members	Baska Formation
		Drug Formation
		Shaheed Ghat Formation

2.3.1 Ghazij Formation

Oldham introduced the term Ghazij in 1990. According to Shah (1999), the Ghazij Formation is mainly comprised of shales along with minor amounts of sandstone, coal, limestone, alabaster, claystone, and conglomerat. Ghazij Group is abundantly found in the Sulaiman basin. Dunghan Formation overlies the Gazij Formation and it is overlaid by Kirthar Formation. It is comprised of three members: Shaheed Ghat Formation, Drug Formation, and Baska Formation.

2.3.1.1 Shaheed Ghat Formation: Sibghatullah Siddiqui (1965) named the Shaheed Ghat Formation to the shales and clays of Rakhi Gaj and the Eames (1952) nodular shales. The type section of Shaheed Ghat Formation is Zindapir, Dera Ghazi Khan District. Lithologically this formation is composed of interbedded fossiliferous clays varying in color from green to brown along with limestone or marl beds. This formation contains nummulitic beds, gastropods, and bivalves. Based on the fossils found in the formation it is assigned with the age Early Eocene.

2.3.1.2 Drug Formation: The Pakistani stratigraphic council chooses the term Drug Formation for the limestone rubble of the Eames (1952). The type locality of this formation is 3km towards the southeast of Drug village. It is composed of off-white to grey color limestone and greenish grey intercalated shales in the lower and middle parts of formation. The formation contains foraminifera, gastropods, and algae in addition to coquina beds and is extremely fossiliferous. Drug Formation is of Early Eocene.

2.3.1.3 Baska Formation: Baska shale was recommended by Hemphill and Kidwai (1973) to take the place of the descriptive term "shale with alabaster" used by Eames (1952). The type section of Baska Formation has exposed about 2km towards the east-northeast of Baska Village. The lithology of this formation consists of greenish shale and clays having fine-textured gypsum having foraminifera, bivalves, and gastropods in it. Foraminifers include Lockartia, Discocycline, and Cuneoline sp. The Baska Formation is categorised into Lower Eocene.

2.3.2 Kirthar Formation

The term Kirthar was used by Blanford (1876) afterwards Kirthar Ranges for Eocene strata. Gaj River is its type locality. It has contact with the Baska Formation on lower side, a member of the Gazij Formation. Members of Kirthar Formation include Drazinda Formation, Pirkoh Formation, Domanda Formation, and Habib Rahi Formation.

2.3.2.1 Habib Rahi Formation: The stratigraphy committee of Pakistan finalized this name to the Habib Rahi Member and Habib Rahi Limestone by Tainsh et al. (1959) and Meissner et al. (1968) respectively. The type locality of this formation is in the vicinity of Dera Bugti town. Habib Rahi Formation is mainly composed of argillaceous limestone having marl and shale in it. Formation contains an abundant amount of Assilina. It is assigned with the age of early to middle Eocene.

2.3.2.2 Domanda Formation: Hemphill and Kidwai (1973) were the first to adopt the word Domanda, which was eventually formally referred to as the Domanada Formation by the Pakistan's stratigraphy committee. The Zhob-Dera Ismail Khan Road is close to the type location of this Domanda Formation. Formation is consisting of claystone, fine to medium-grained sandstone, and calcareous mudstone. It contains bivalve, gastropods, foraminifera, echinoids and some vertebrate fossils. It is assigned the middle Eocene age.

2.3.2.3 Pirkoh Formation: Eames (1952) white marl band was named Pirkoh suggested by Hemphill and Kidwai (1973). The type locality of Pirkoh Formation is the Pirkoh anticline. This formation is made of limestone, shale, and marl. On the base of gastropods, bivalves, foraminifera, and echinoids found in the Pirkoh Formation it is designated as middle Eocene in age.

2.3.2.4 Drazinda Formation: Hemphill and Kidwai (1973) first used the term Drazinda shales. The type locality of the Drazinda Formation is east and northeast of the Drazinda village. It is composed of shale, fossiliferous marl, and mud. Drazinda Formation is highly fossiliferous, and its fauna consists of bivalves, foraminifera, and bivalves. Its age is the late middle Eocene.

Age		Formation		Description	Thickness	Lithology
Quaternary	Holocene	Recent Deposits		Alluvium, Meander Belt, Active Flood and Dune Sand Deposits	2000m	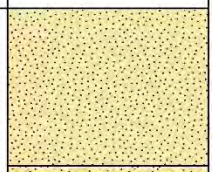
		Sub-recent Deposits		Flood plain, Sub Piedmont, Piedmont, Alluvial Fan and Terrace Gravel Deposits		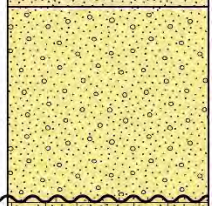
	Pleistocene	Dada Conglomerate		Light brownish grey, massive conglomerate, boulders, cobbles, pebbles of sandstone and limestone	9m	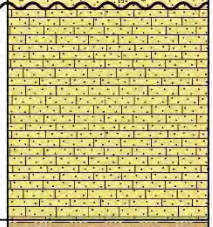
Neogene	Pliocene	Siwalik Group	Chaudhwan Formation	Massive conglomerate with sandstone and clay	+1422m	
			Litra Formation	Sandstone with minor clay	+2002m	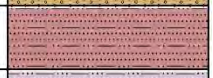
			Vihowa Formation	Claystone with sandstone	+975m	
Paleogene	Oligoene Miocene	Chitarwata Formation		Sandstone with siltstone	320m	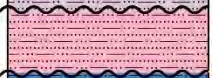
	Eocene	Drazinda Formation		Shale with siltstone	583m	
		Pirkoh Formation		Limestone	19m	
		Domana Formation		Claystone/shale	460m	
		Habib Rahi Formation		Limestone	74m	
		Baska Formation		Shale and limestone	277m	
		Drug Formation		Limestone	345m	
		Shaheed Ghat Formation		Shlae with intercalated siltstone and limestone	1870m	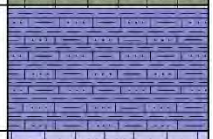
	Paleocene	Dungan Formation		Limestone	211m	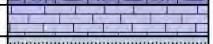
		Rakhi Gaj Formation		Shale intercalated sandstone	357m	

Figure 2.2: Stratigraphy of Zindapir Anticline

CHAPTER 3

Field Observation

Detailed geological field observations conducted on the Drug Formation along the Zindapir Anticline area of Dera Ghazi Khan, Pakistan, which have yielded significant findings regarding its lithological characteristics, sedimentary structures, and variations seen in outcrop level. Substantial information of the litho-units, depositional environment, diagenesis, and regional geological context of the formation was gained as a result of the extensive fieldwork, which also included thorough measurement of the exposed outcrop, the thickness of each bed and rock sampling from each bed. Fieldwork-based structural investigations shed light on the tectonic history and deformational processes that impacted the Drug Formation. The formation is part of the renowned regional fold known as the Zindapir Anticline, which has an asymmetric geometry. The anticline has a sharply descending hinge, which denotes strong compressional pressures that caused the rock strata to fold. The beds of the Drug Formation are observed to drop towards the anticline's center, following the geometry of the folds.

Massive limestone beds with irregular shale intercalations make up the majority of the Drug Formation. The color of the limestone strata varies, ranging from yellowish to off-white to grey. The formation's thickness, as determined by field measurements, is around 358 meters. The higher units of the exposed strata mostly consist of heavily bedded limestone with minor shale layers, the lowest portion of the formation is composed of rather thick bedded shales. The limestone found in the Drug Formation demonstrates a number of remarkable lithological characteristics. Nodularity is one of the distinguishing features, which denotes the existence of diagenetic processes that result in the formation of nodules or concretions within the rock matrix. These nodules, which can vary in size, shape, and distribution, are thought to have developed as a result of mineral precipitation in the aftermath of pore fluid chemistry alters during diagenesis. Nodularity in the lower beds are more visible as that can observe on lower 3 beds (Figure 3.1 B, C & E) moving upward nodularity started to falter and beds started to become less nodular (Figure 3.1 F, H, I & M-O). The presence of blocky calcite and clear calcite veins in the limestone strata is another distinguishing characteristic. These veins show instances of post-depositional mineralization, where fluids with high concentrations of dissolved calcium carbonate ($CaCO_3$) moved through cracks or pore spaces and precipitated calcite crystals. These veins shed important light on fluid flow patterns and mineralization processes that took place in earlier geological periods. The Drug Formation has an extensive

and varied fossil record, which suggests a rich paleontological history. The limestone matrix frequently contains a variety of bioclasts, including brachiopods, bivalves, and skeletal grains. These fossils indicate that the formation was likely formed in a marine environment, where a variety of animals flourished and left behind their remnants. Bioclast diversity and distribution patterns can reveal important details about the region's paleoecology, paleoenvironment, and paleoclimate at the time of deposition. The formation's outcrops have been meticulously mapped to demonstrate changes in bedding attitudes.

Additionally, the contact interactions between the Drug Formation and the other strata shed light on the regional geological context and stratigraphic succession. The change from carbonate-dominated sedimentation to more clay-rich circumstances is marked by the formation's lower contact with the Shaheed Ghat Formation, which is composed of clays with limestone and marl. Another boundary that indicates a transition to shale-dominated depositional settings is the upper contact with the Baska Formation, which is composed of gypsum-bearing shales. These connections help to relate the formation to other rock units in the area and show variations in depositional environmental circumstances. Nodularity, calcite veins, and other diagenetic characteristics can shed light on fluid flow patterns and post-depositional activities. These findings may be used to characterize reservoirs and comprehend fluid movement routes in hydrocarbon exploration and production.

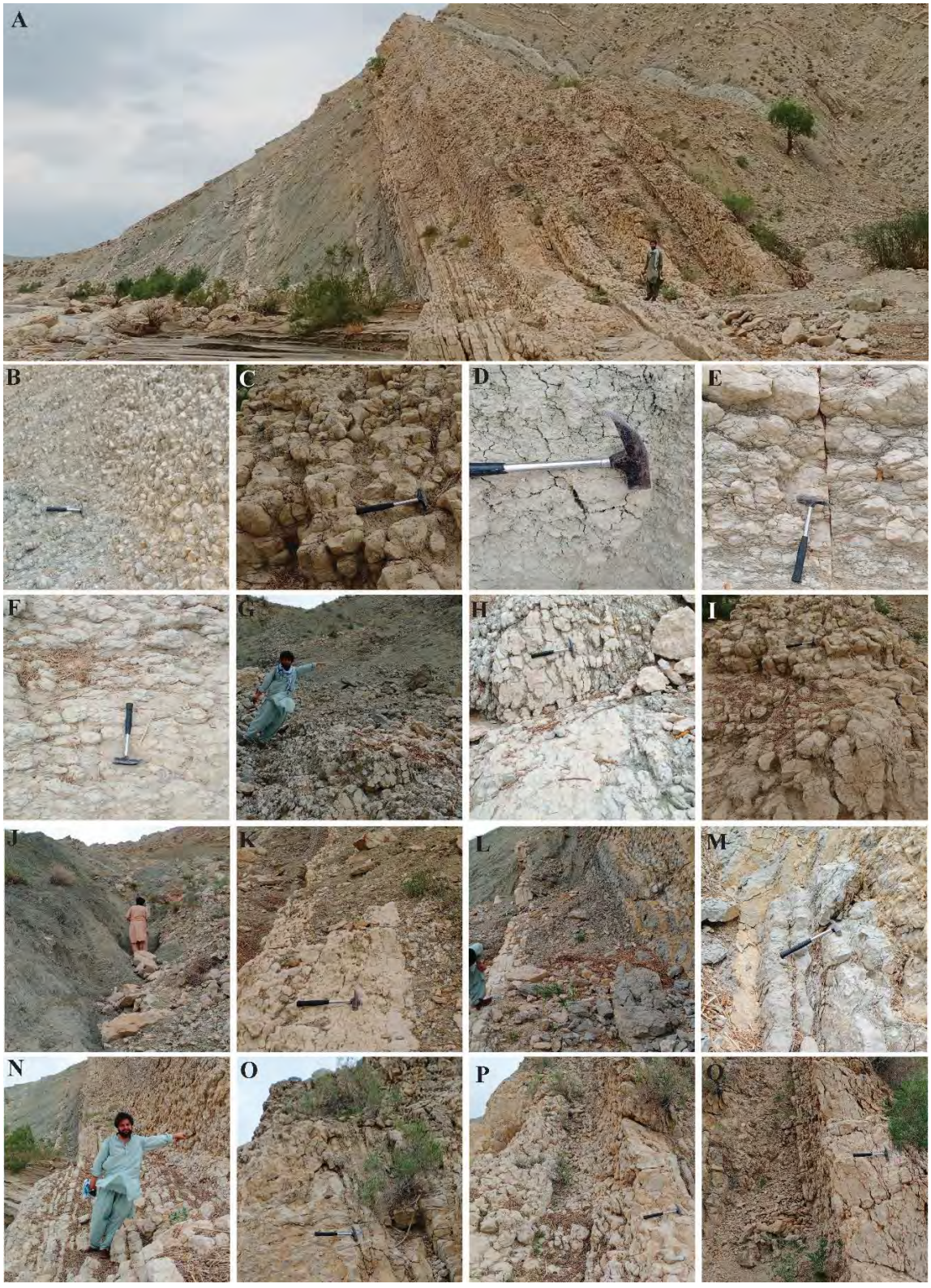

Figure 3.1: Field photographs. A: Panoramic view of Drug Formation. B and C show high nodularity. B-Q: Close view of studied sections (includes Limestone beds having high to moderate nodularity and greenish shale in G and J)

CHAPTER 4

Research Methodology

4.1 Field work

A detailed field investigation was conducted along the Zindapir Anticline, focusing on identifying a well-exposed section of the Drug Formation. After careful examination, a suitable location was chosen in the Zindapir section, which offered maximum exposure of the Drug Formation and clear demarcation of its upper and lower contacts. This selection ensures accurate sampling and comprehensive data collection for further analysis and interpretation.

During the fieldwork, precise measurements of the Drug Formation were taken, providing an actual thickness of 356m with well-developed upper and lower contact with Shaheed Ghat Formation and Baska gypsum member of Ghazij Formation. The formation was then carefully examined and divided into distinct lithological units based on several criteria, including lithology, nodularity, grain size, texture, fossil content, and bedding size. This systematic approach allowed for the identification of 18 lithofacies, which were marked from the lower to the upper part of the formation, capturing the variations observed in the outcrop.

Sampling collection is the most fundamental and important part of carbonate microfacies analyses and study of diagenetic overprints. Total of 21 samples were collected in systematic way for microfacies analyses, covering the entire vertical extent of the formation, from the bottom to the top, which covers the wide range of variation to construct the paleoecology and depositional setting based on biota assemblages. Similarly, the representative samples for study of diagenesis phases are collected based on the diagenetic events observed at outcrop scale, such as various calcites, fractures, suture seems, dolomitization events and fabric selected dissolution.

4.2 Petrographic studies

The selected samples were transported to the rock cutting lab at the Earth Sciences department of Quaid-i-Azam University in Islamabad for further analysis. In the lab, the field samples underwent a series of preparation steps to create thin sections suitable for petrographic studies. Initially, the samples were cut in different orientations, and the desired orientation for analysis was carefully selected. This step ensured proper attachment between the glass slide and the rock slice. After the attachment of the rock slice to the glass slide using epoxy resin, further grinding and polishing were performed to achieve a thickness of up to 30 microns for

the preparation of thin sections, making sure the surface is smooth and even. This thickness allows for optimal light transmission and detailed examination of the sample under a microscope. The chosen rock chips were then subjected to a polishing process using 1000# silicon carbide polishing powder.

The prepared thin section slides were then studied using a Leica DM750P microscope equipped with a DFC290 digital camera. The Leica application suite software was utilized to capture high-quality images and facilitate analysis and documentation of the thin sections. This microscopy setup provides the necessary magnification and resolution to observe and document the microfacies, their variations, and unravel the diagenetic overprints within the Drug Formation. This analysis will contribute to a comprehensive understanding of the formation's sedimentary characteristics, diagenetic history, and reservoir potential.

4.3 Plug Analysis

After the petrographic investigation, the selected samples underwent further testing to assess their porosity and permeability characteristics. The sample selection was based on the textural variation observed in the depositional facies of the Drug Formation. In total, four samples were chosen for the air porosity and permeability analysis. This normalization helps in quantifying the pore volume available for fluid flow within the reservoir. Furthermore, based on the porosity values obtained, the reservoir quality index (RQI) and reservoir flow zone index, a comprehensive understanding of the reservoir properties and flow characteristics of the Drug Formation can be obtained. These parameters are essential in determining the commercial viability and production potential of hydrocarbons within the formation.

4.4 Source rock evaluation

Selected samples were investigated to find the source rock potential. The Total Organic Carbon (TOC) content of the samples was analyzed to determine the organic richness of the rocks. Samples with high TOC values indicate a higher potential for hydrocarbon generation. To further assess the hydrocarbon generation potential, the rock evolve pyrolysis technique was employed. This process involves subjecting the samples to controlled heating under specific conditions. During rock evolve pyrolysis, various parameters are measured, including S1, S2, and S3. Where, S1 represents the measurement of free hydrocarbons released during pyrolysis, indicating the presence of organic matter that can generate hydrocarbons. S2 indicates the amount of hydrocarbons generated through thermal cracking of the organic matter. S3 represents the measurement of carbon dioxide (CO_2) released during pyrolysis. The

T_{max} value is also measured during rock evolve pyrolysis. T_{max} represents the temperature at which the organic matter reaches its maximum rate of thermal decomposition. It provides insights into the maturity level of the organic material and the potential for hydrocarbon generation. The derivatives of later parameters are also measured to designate the source rocks quality genetic potential, generative potential and the maturity level.

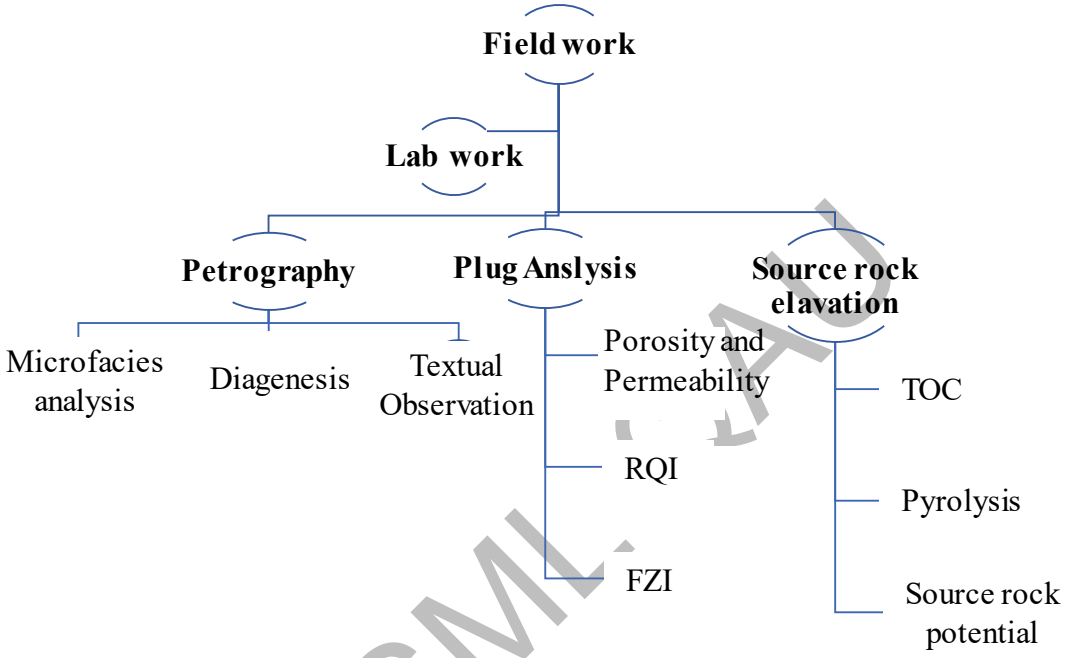

Figure 4.1: Flow Chart of Methodology

CHAPTER 5

Microfacies Analysis and Diagenesis

5.1 Microfacies Analysis

The microfacies analysis tells us that Drug Formation in the Zindapir Anticline deposited in the inner shelf environments. The inner shelf environment is further divided into tidal, lagoonal, back-reef, reef-patch, and fore-reef environments (Boudaugher-Fadel, 2018).

5.1.1 Tidal Environment

5.1.1.1 Dolomitic Lime Wakestone to Packstone - MF1

This facie can be found in the lower part of the Drug Formation stratified at the area of 7m. It is composed of greenish-grey compacted limestone with a small amount of marly content. At the outcrop scale the facie displays a high density of fracture and various calcitization phases cross-cutting each other, and low to moderate dissolution is observed in places (Figure 5.1C&D). The dolomite is euhedral in places and mostly subhedral to anhedral texture in the micritic lime mud matrix (Figure 5.1A). Mg-rich fluids passing through the veins cause dolomitization (Figure 5.1C).

Interpretation: The thin section study of this dolomitic lime wackestone to packstone microfacies has scattered sparry calcite. This facies displays depositional settings on the inner shelf, low energy, confined flat tidal settings (Wilson, 1975). Another indication that the lime was subjected to the dolomitization process is the presence of fine-crystalline dolomite in it, an indication of inner shelf environments. This facies is interpreted to be found in tidal environments. The dolomitization phenomena associated with lime mud texture is the early diagenetic phase (Wanas, 2008).

5.1.2 Lagoonal Environment

5.1.2.1 Mullascan Wackestone - MF2

Mullascan Wackestone is present in the middle part of the Drug Formation, exhibiting a thickness of 8 meters, composed of thickly bedded offwhite limestone. Petrographic analysis shows that this microfacies is composed mainly of articulated or inarticulated mullascans shells

(Figure 5.2). Millolids, austrotrillina and some nummulites and algaes are also found in this microfacies. The original bioclast is replaced by blocky calcite (Figure 5.2 A&B).

Interpretation: Based on the profusion of the compact micritic matrix, the availability of fauna, and borrowing, this facies indicates deposition in planktic foraminifera, which suggests a shallow lagoonal setting with low energy conditions (Abd El-Moghny and Afifi, 2022). The miliolidae and coarse sparry calcite groundmass, along with the moderately sorted texture of the fully preserved bioclastic allochems, showed that this microfacies type was deposited in a shallow marine, more limited shielded lagoonal setting (Sallam et al., 2015).

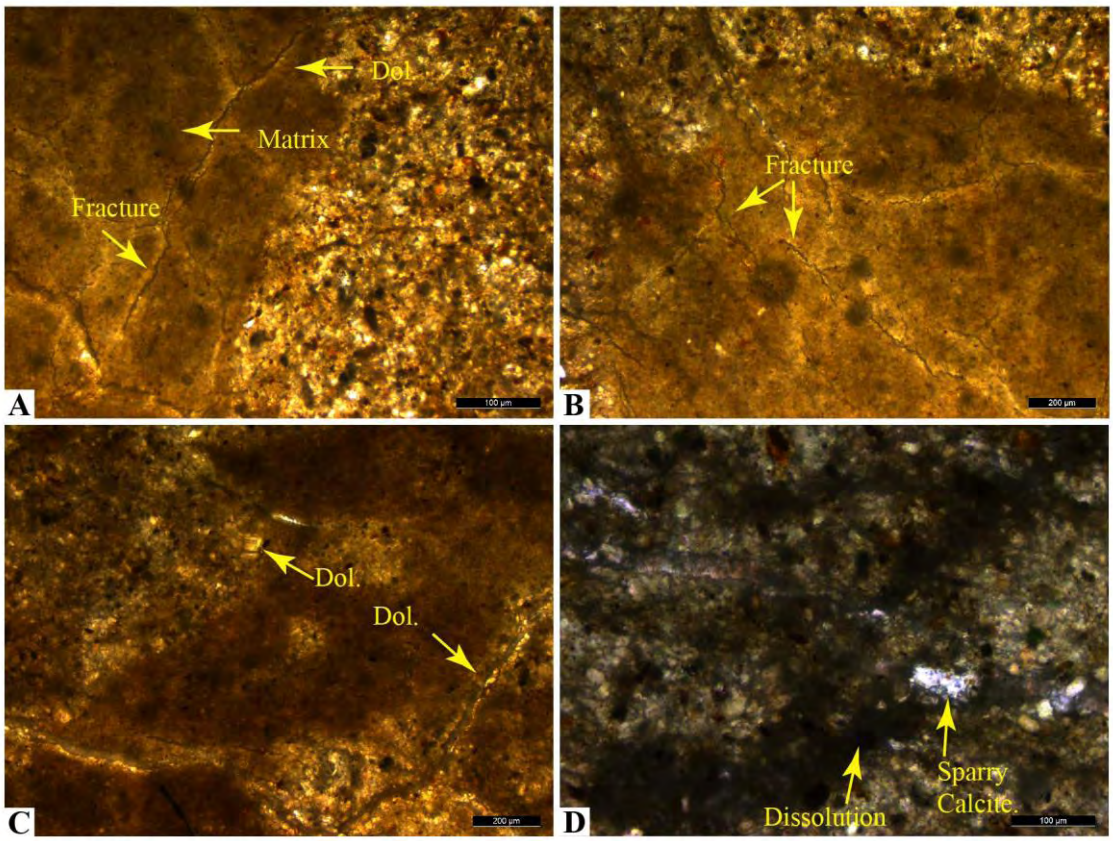

Figure 5.1: Dolomitic Lime Wakestone to Packstone (MF1) showing fractures in A & B. D shows Dissolution and sparry calcite. Dol.= Dolomite

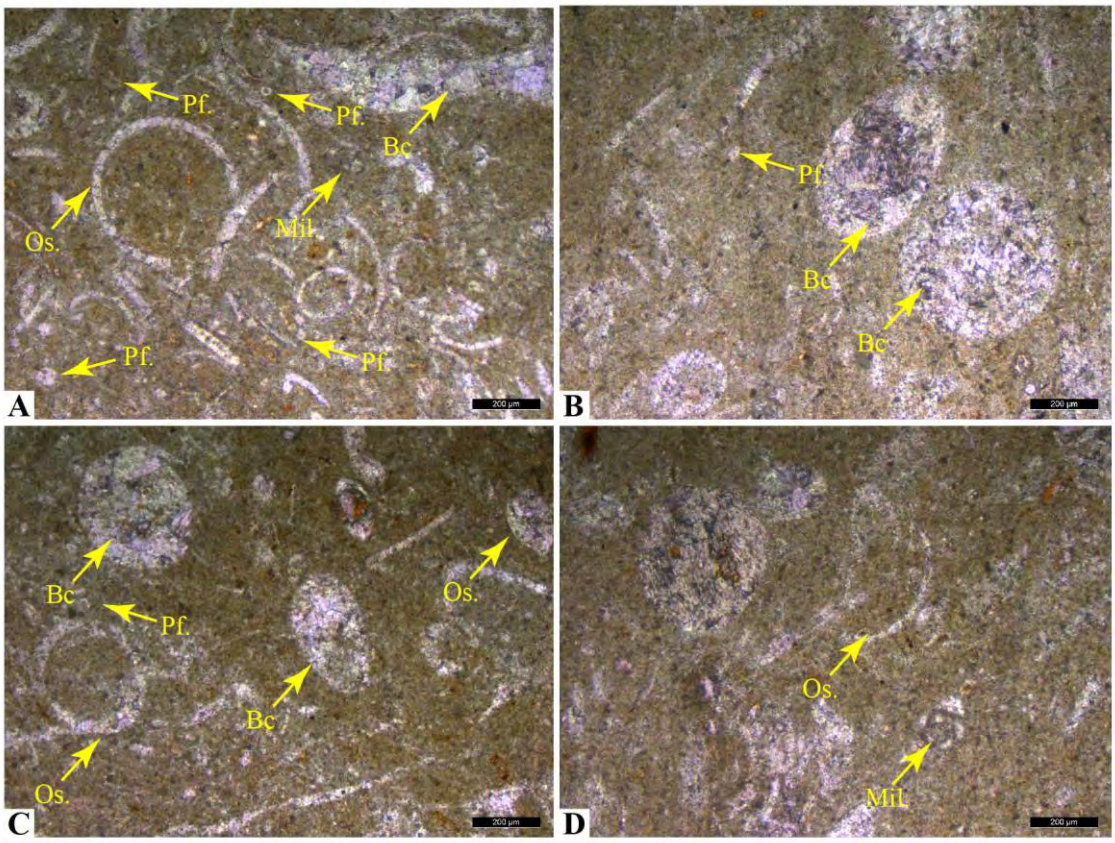

Figure 5.2: Mullascan Wackestone (MF2) shows an abundance of bioclast Os.= Ostracod shells, Pf.= Planktic Foraminifera, Mil= millolids, Bc= Blocky calcite.

5.1.2.2 Miliolid Bioclastic Wakestone to Packstone - MF3

This facies was reported in the upper part of the Drug Formation, showing a thickness of 6m. Petrographic analysis of this microfacies display articulated and/or unarticulated bioclast along with smaller millolids, astrotrilina, and very low planktonic foraminifers (Figure 5.3). This facies also has telogenetic calcite (Figure 5.3D). Other minor content includes shallow benthic foraminifera i.e., Lockhartia and rotalida sp, and oysters in very minor amounts.

Interpretation: Porcelainous miliolid foraminifera is found in shallow nearshore and lagoonal habitats down to a depth of around 50 m. Shallow marine settings lack or have few planktonic foraminiferas (Flügel, 2004). The deposition is evident from the micritic matrix, which is considerably below the fair-weather wave base (Babazadeh & Alavi, 2013). This microfacies is also mud dominant indicating low-energy conditions (Wilson, 1975; Burchette and Wright, 1992). The coarser sparry calcite groundmass, many miliolidae that are sparite-filled, and the moderately sorted, preserved bioclasts supported the shallow marine, more protected lagoonal environment (Sallam et al., 2015).

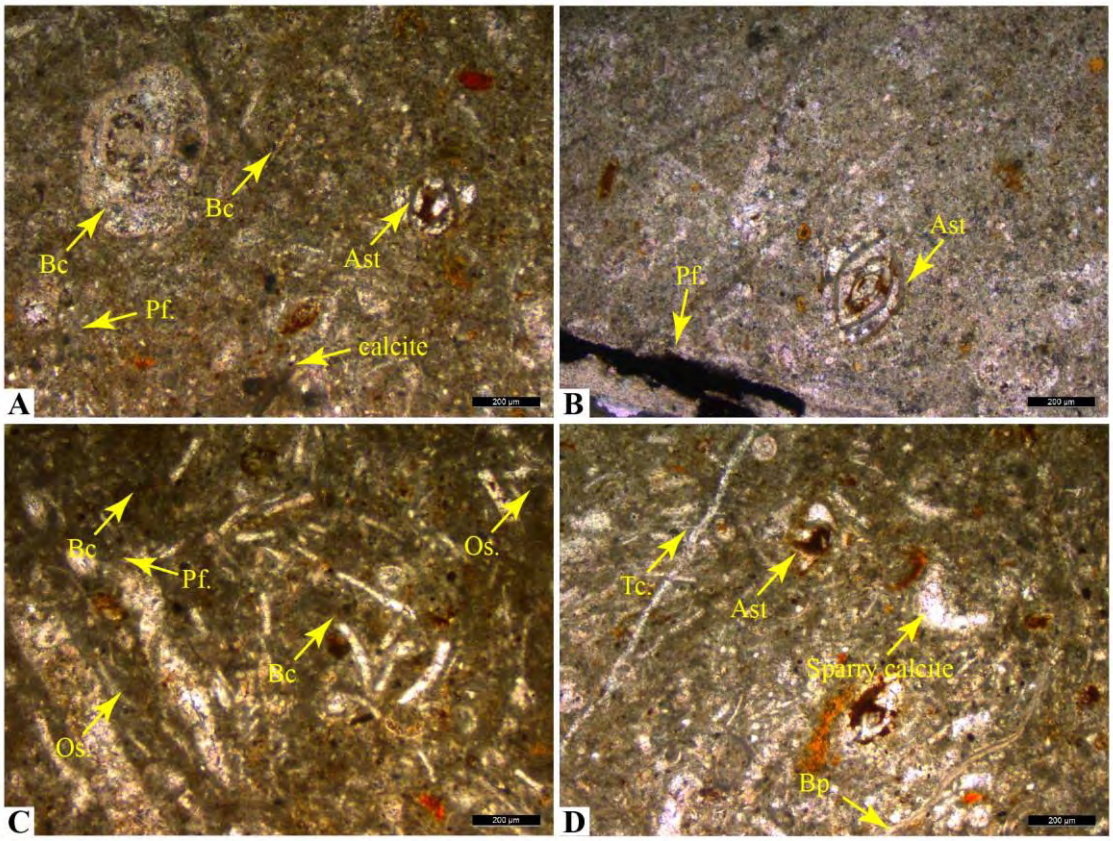

Figure 5.3: Miliolid Bioclastic Wakestone to Packstone (MF3) Bc=Bioclast, Pf.= Planktonic Foraminifera, Ast= Austrotrillina, Os.= Ostracod shell, Tc= Telogenetic Calcite, Bp= Brachiopod shell fragments.

5.1.2.3 Brachiopoda Nummulitic Grainstone - MF4

Brachiopoda Nummulitic Grainstone deposited in the upper part of the Drug Formation, having a thickness of 1m. It is composed of nodular limestone beds. This microfacies contain 40% allochems, which include a large number of nummulites. Other allochems are preserved fibrous brachiopod shells (10%), miliolids (< 5%), Austrotrillina, and sparry calcite (Figure 5.4).

Interpretation: Nummulites that relocated from a closer reef patch remained well-preserved, due to the lagoon's low energy condition, while some got damaged during transport. This facies is mud supported representing a low-energy environment (Wilson, 1975; Burchette and Wright, 1992). A shallow marine, the more confined sheltered lagoonal environment was proved by the miliolidae with sparite-filled chambers, well conserved and moderately sorted bioclasts, the coarse sparry calcite groundmass (Sallam et al., 2015). Well-preserved ostracod, nummulites, accompanied by austrotrillina formed in back-reef to open lagoonal settings with minimal hydrodynamic energy during the Oligocene and Early Miocene (BouDagher- Fadel et

al., 2000). Milliods support the distal part of the back reef environment, and the low energy level and limited circulation enable sparry calcite to precipitate. This facies are interpreted to be deposited in the distal back reef to open lagoonal settings. Overall, the dominance of Autrotrilina with sparry calcite signifies to backreef environment (Roozpeykar & Moghaddam, 2016).

5.1.2.4 Millolid Wakestone - MF5

Millolid wakestone microfacies is present at the upper part of the Drug Formation. Exhibiting thickness of 6m, consisting of nodular limestone beds. This microfacies have millolids (30%), and another biota comprises of nummulites, and mullascan shell fragments (Figure 5.5). The petrographic study of this microfacies implies that the bioclast and shallow marine faunal texture is vanished due to extreme diagenesis. However, in places, the austrotrilina and some very minor planktonic foraminifera is slightly preserved (Figure 5.5 A).

Interpretation: The presence of millolid foraminifers indicates restricted muddy inner platforms most probably lagoon (open/restricted) (Flügel, 2004). This microfacies is typically from lagoonal, low-energy settings based on the marker shallow benthic milliolida genus austrotrillina which is present throughout the litho-unit (Wilson, 1975; Burchette and Wright, 1992).

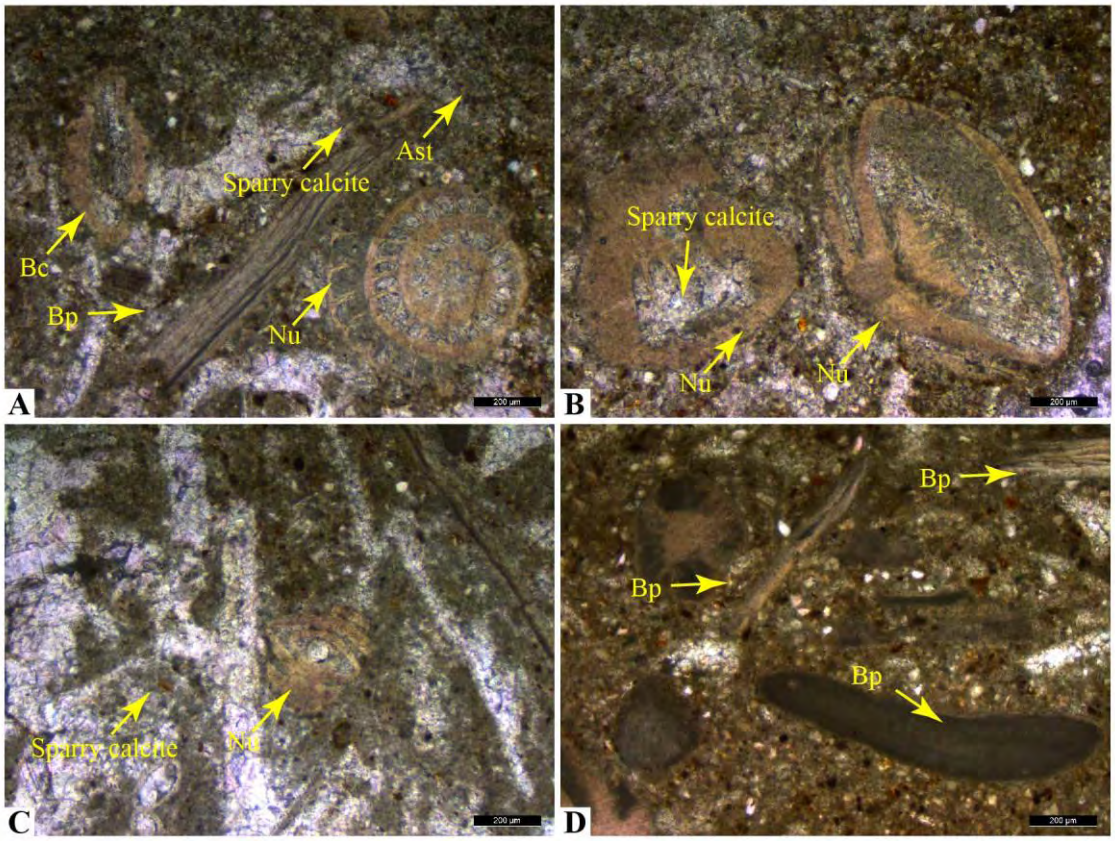

Figure 5.4: Brachiopoda Nummulitic Grainstone (MF4) Bc= Bioclast, Bp= Brachiopod Shell, Ast= Austrotrilina, Nu= Nummulites.

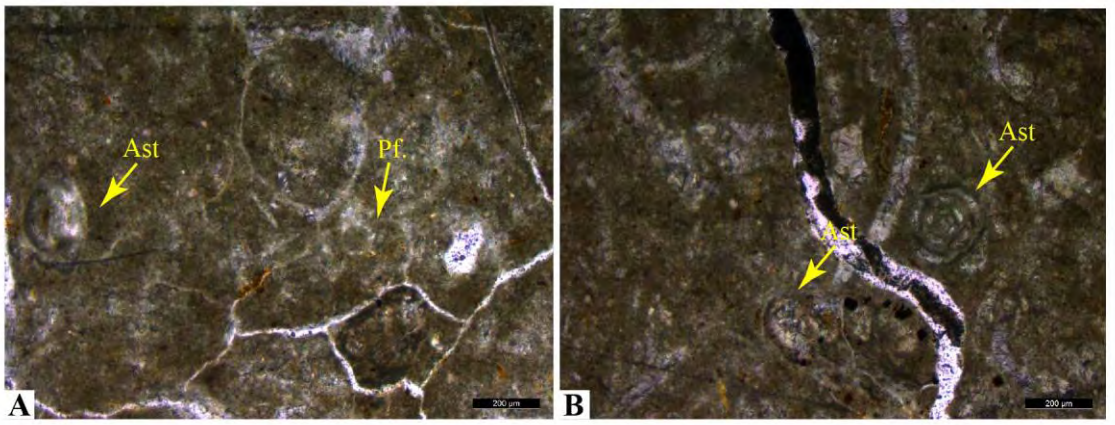

Figure 5.5: Millolid Wakestone (MF5). Ast= Austrotrilina, Pf.= Planktic Foraminifera.

5.1.3 Back-Reef Environment

5.1.3.1 Miliolid Nummulitic Ostracodal Wackestone - MF6

Miliolid nummulitic ostracodal wackestone microfacies found in the lower part of Drug Formation. It is comprised of nodular limestones; nodules are slightly bigger in size as compared to the entire nodularity in the exposed outcrop section, which is intercalated with marl and calcareous material. This microfacies has a thickness of 20m and comprised of ostracodal shells, miliolids, austrotrilina, and nummulitic species; N. atacicus, and N. mammilatus. The petrographic analysis also revealed sparry calcite and minor euhedral dolomite rhombs in places (Figure 5.6).

Interpretation: Contemporary millolids thrive on a soft substrate in shallow, restricted habitats with slight agitation. (Davies,1970; Brasier, 1975a; Geel, 2000). Austrotrillina nurtures symbiotic algae. It also accompanied well-preserved ostracods and nummulites in extremely low hydrodynamic energy on distal back reefs throughout the Oligocene and Early Miocene. (BouDagher- Fadel et al., 2000).

5.1.3.2 Nummulitic Mulluscan Packstone - MF7

Nummulitic mulluscan packstone is also found in the lower part of Drug Formation stratified on 12m. This facies is composed of light grey limestone having stretched nodules also intercalated with shales. The primary composition of the facies is the molluscan assemblage. Other identified microfossils are orbitolites, millolids and rotalidae (rotalidae trochidiformis), nummulities and small millolids (Figure 5.7).

Interpretation: The abundance of coarse-grained molluscan and nummulites indicates a primarily back reef, open lagoonal depositional environment (Tucker, 2001). The unusual density of orbitolites and millolids identify typical of a back reef environment, and the presence of mud is also favoring low energy conditions (Wilson, 1975; Burchette and Wright, 1992). Similarly the presence of orbotolies also supports the backreef shelf depositional setting of the facies (Boudaugher-Fadel, 2018).

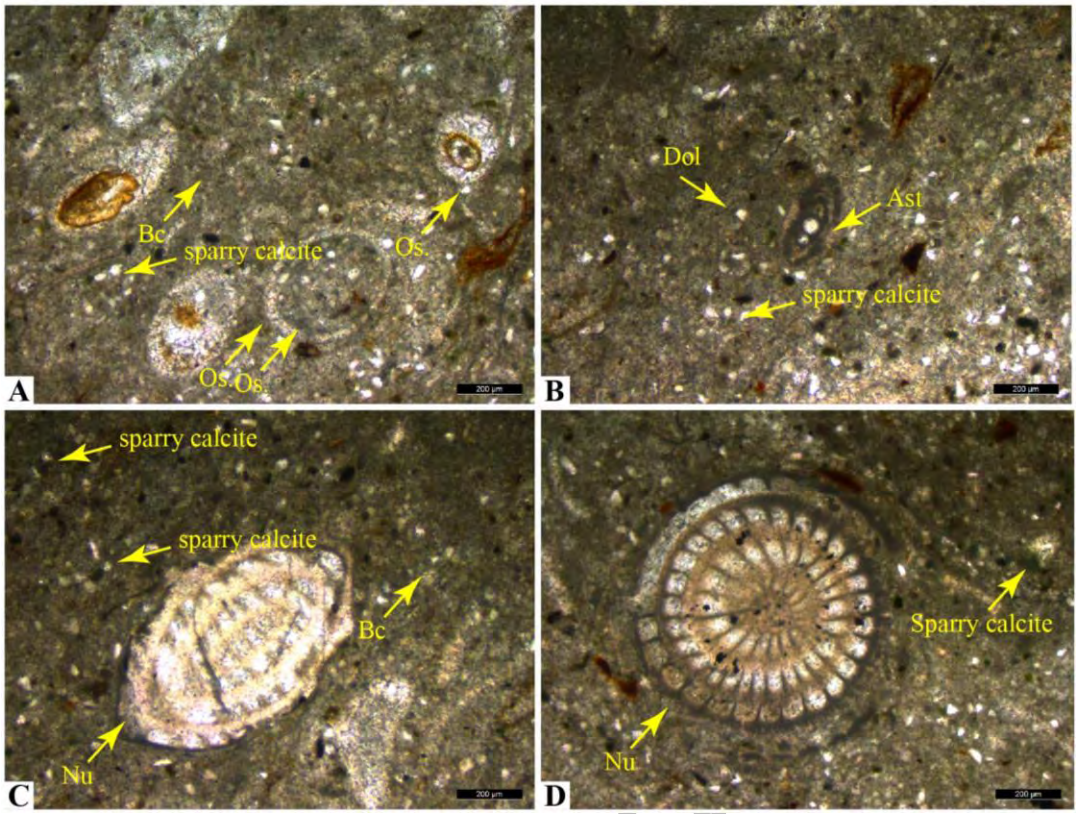

Figure 5.6: Miliolid Nummulitic Ostracodal Wackestone (MF6). Bc= Bioclast, Os.= Ostracod shell, Dol= Dolomitic rhomb, Ast= Austrotrilina, Nu= Nummulitic sp.

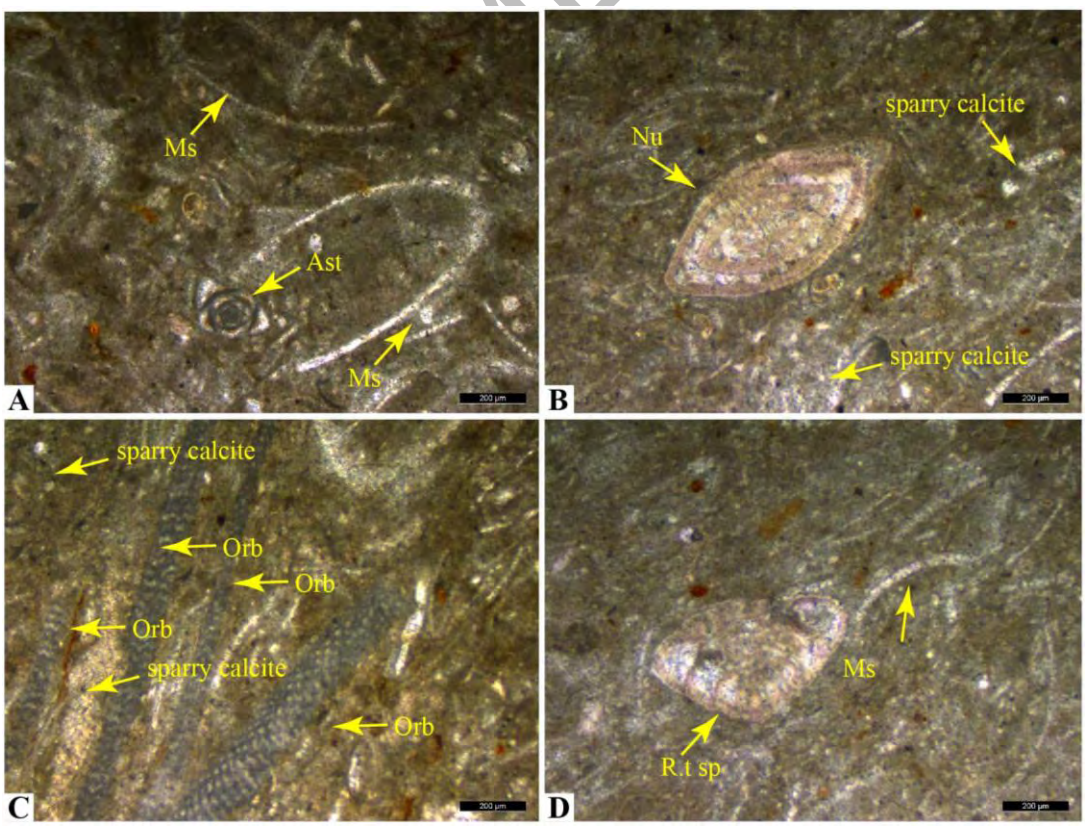

Figure 5.7: Nummulitic Mulluscan Packstone (MF7). Ast= Austrotrilina, Ms.= Mullascan Shell, Nu= Nummulities sp., Orb= Orbitolites, R.t= Rotalid Trochidiformis.

5.1.3.3 Milliolid Nummulitic Grainstone - MF8

Miliolid nummulitic grainstone is distributed in various parts of the Drug Formation, having a thickness of 7 to 8 meters for each bed and composed of light yellow thick-bedded limestone beds intercalated with marl at some places. This microfacies was developed in the lower and upper parts of the Drug Formation; having contact with Baska Gypsum. Petrographic analysis shows well-preserved nummulities and ostracodal fragments along with blocky calcite. Minor content of includes gastropods, broken bioclast fragments and smaller millolids (Figure 5.8).

Interpretation: The coexistence of numerous nummulites, bioclasts, and millolid in this microfacies indicate that it was formed in low energy and shallow water environment in the distal back reef on an inner shelf (Mirza et al., 2022). Well-preserved ostracod, nummulites, accompanied by austrotrillina formed in back-reef with minimal hydrodynamic energy during the Oligocene and Early Miocene (BouDagher- Fadel et al., 2000). The mud dominancy in this facie is also supporting low energy conditions (Wilson, 1975; Burchette and Wright, 1992).

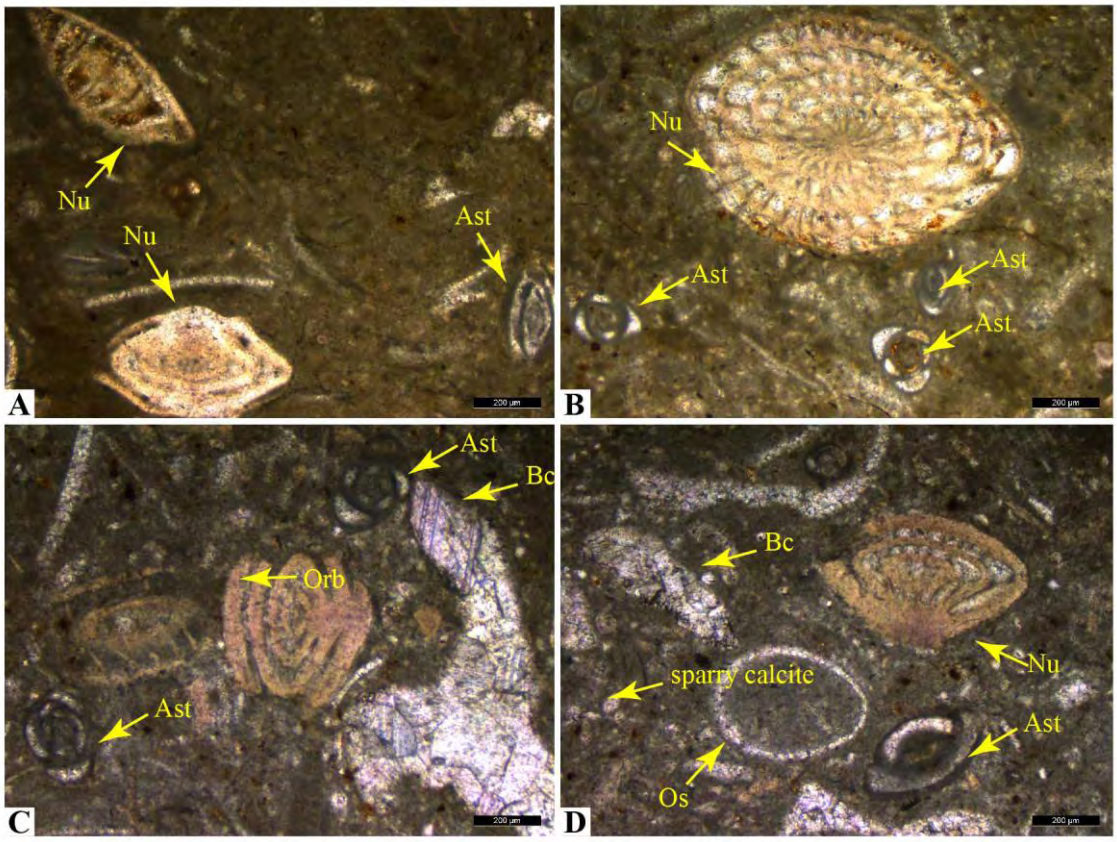

Figure 5.8: Milliolid Nummulitic Grainstone (MF8). Nu= Nummulitic sp., Ast= Austrotrilina, Bc= Blocky calcite, Os= Ostracod shell.

5.1.3.4 Miliolid Mulascan Algal Grainstone - MF9

This microfacies is found in the middle of the Drug Formation having a thickness of 15 meters. It is composed of offwhite nodular limestone beds. This microfacies is mainly composed of algae along with mullascan shells, gastropod shells, bilvalves, austrotrillina, millolids, and some nummulites (<15%) also appeared in this facies (Figure 5.9).

Interpretation: The reported faunal content and the slightly sorted, larger bioclastic, algaes, and ostracods, along with the micritic matrix, suggest the distal part of back-reef to open lagoonal environment (Abd El-Moghny and Afifi, 2022). The mud dominance and presence of the austrotrillina, well-preserved ostracod and milliolids, and abundance of calcareous algae represent low hydrodynamic energy back-reefs (BouDagher- Fadel et al., 2000; Wilson, 1975; Burchette and Wright, 1992).

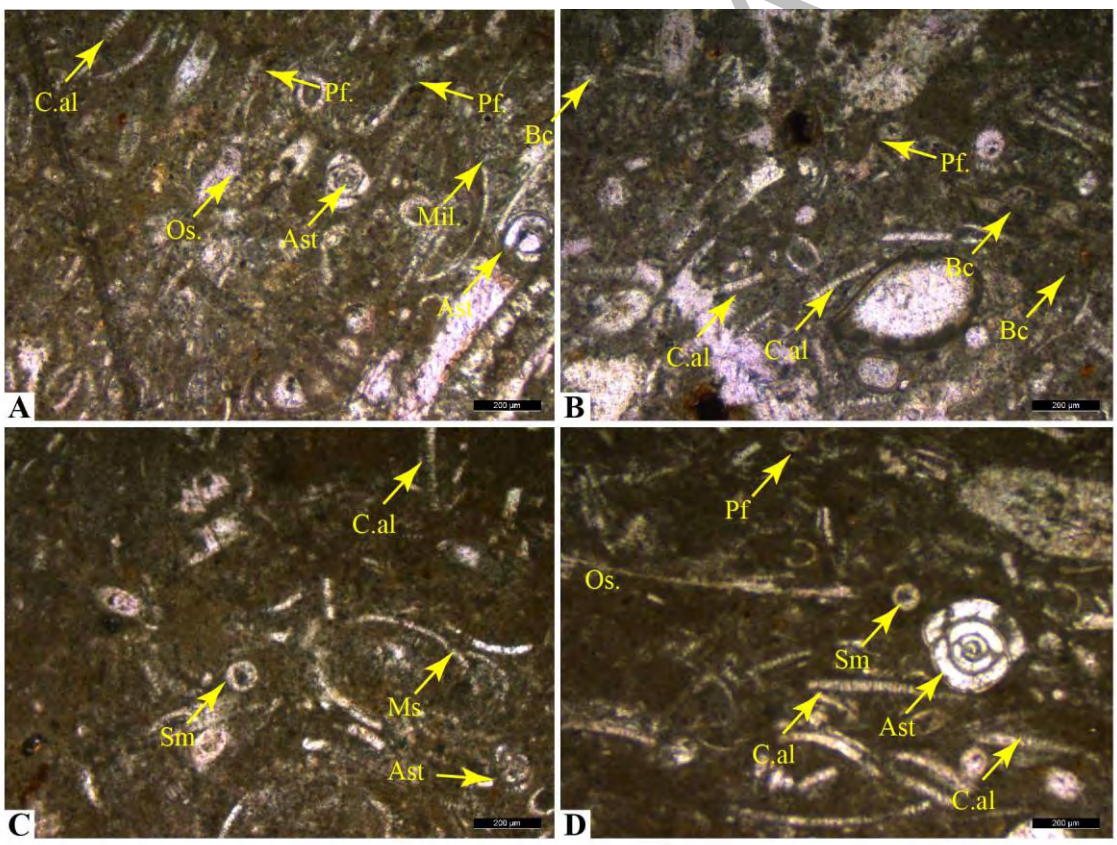

Figure 5.9: Miliolid Mulascan Algal Grainstone (MF9). C.al= Calcarious Algae, Pf.= Planktic Foraminifera, Mil.= Millolid, Ast= Austrotrillina, Os.= Ostracod, Sm= Small Millolid

5.1.4 Fore-Reef Environment

5.1.4.1 Nummulitic Ostrocodal Bioclastic Wackestone - MF10

Nummulitic ostrocodal bioclastic wackestone is present in the Drug Formation's lower part, exhibiting a thickness of 15 meters. It marked a lower transitional contact of Drug Formation with Shaheed Ghat Formation. It has offwhite limestone along with green shales; limestone shows nodularity along the whole bed. This wackestone microfacies contains abundant ostracod shells (30-35%), bioclast (50%), and nummulites (Figure 5.10). Bioclast is composed of gastropods, broken fragments of ostracods, nummulites including N. vascus and N. atacicus. It has calcite veins filled with blocky calcite (Figure 5.10C).

Interpretation: The primary elements of this microfacies are ostracods and cemented bioclasts reported in freshwater, brackish water, and marine habitats (Flugel, 2004; 2010). Fine matrix with well-preserved ostracods indicates in-situ deposition in low energy conditions. Ostracods are found in a wide range of environments. But Ostracods assemblages with components such as benthic foraminifers shows marine environment. Round to elliptical and flat nummulites are abundant in tropical mesophotic zones (Mateu-Vicens et al., 2012, Pomar et al., 2017). So this facies is interpreted to be deposited on the basal part of the fore-shelf of the inner shelf.

5.1.4.2 Assilina Nummulitic Wakestone - MF11

Nummulitic wakestone microfacies is stratified on the area of 83 meters in the middle to lower part of the Drug Formation. Petrographic analysis revealed well-preserved numulities and Assilina in the thin section (Figure5.11).

Interpretation: The coexistence of the micrite matrix and perfectly conserving biota suggests low energy settings. (Wilson, 1975; Burchette and Wright, 1992; Boudaugher-Fadel, 2018) In a micritic matrix, the prevalence of nummulitids and the lack of alveolinids and orbitolitids imply deposition much below favorable environments. (Eichenseer and Luterbacher ,1992). Nummulites accompanied by assilinas were allocated to habitats on the deep or shallow water shelf. Small lenticular nummulites and ssilinas in large quantities are an indication of shallow water facies in shallow shelf settings, post presumably fore-reef (Ghazi, 2014).

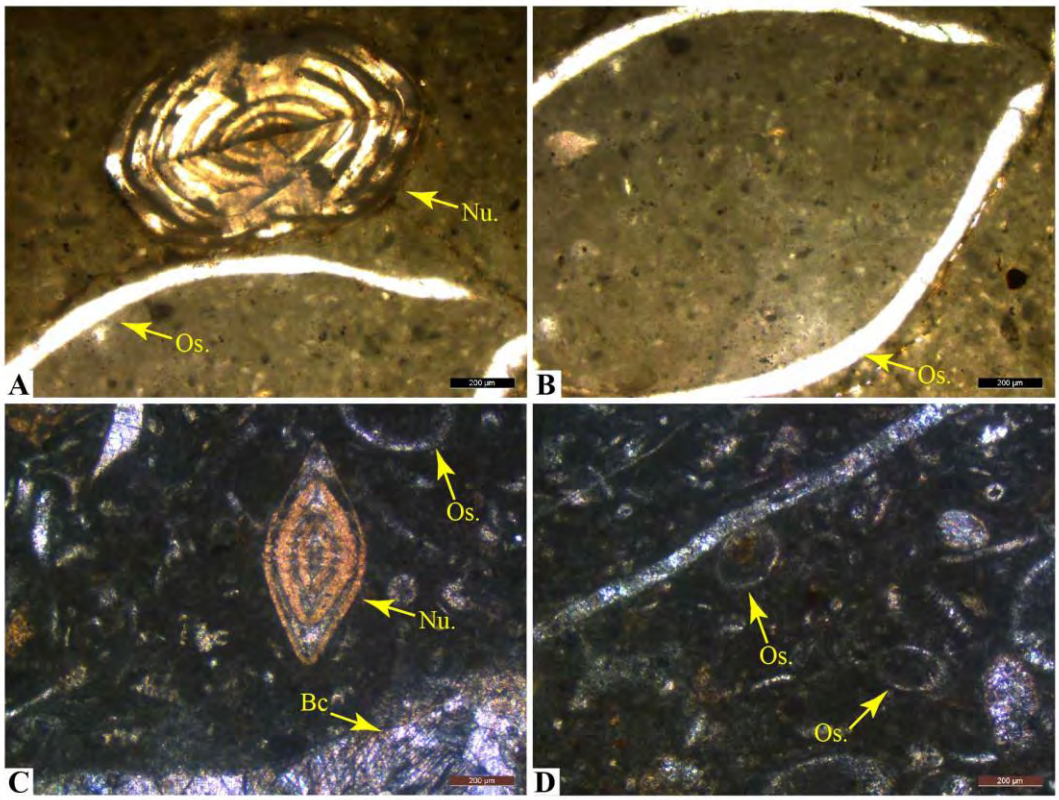

Figure 5.10: Nummulitic Ostrocodal Bioclastic Wackestone (MF10). Os.= Ostracod shell, Nu.= Nummulite sp., Bc.= Blocky Calcite

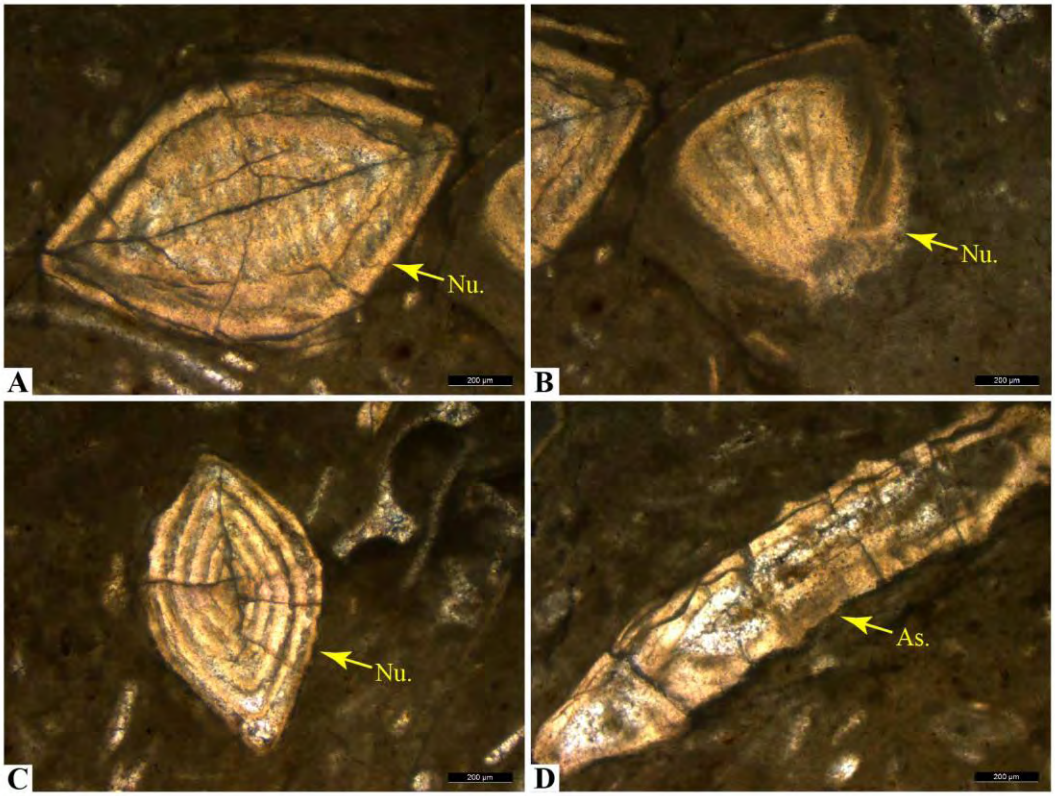

Figure 5.11: Assilina Nummulitic Wakestone (MF11). Nu.= Nummulite sp., As.= Assilina sp.

5.1.4.3 Coralline Nummulitic Bioclast Packstone - MF12

This facies is found in the lower part of the Drug Formation, exhibiting a thickness of 6 to 12 meters. It is composed of yellowish calcareous limestone beds. Microfacies analysis shows amphistegina, broken bioclasts, well preserved in situ nummulitic deposition. Other includes orbitolites, rotalidae, ostracods and minor gastropods (Figure 5.12).

Interpretation: According to Nebelsick et al. (2005), the presence of coralline algal limbs is a typical characteristic of inner shelf environments. As per Sarkar (2015), coralline algae habitats from inner to middle shelf settings, while in their crustose form, are indicative of a middle shelf habitat. Bassi and Nebelsick (2010) determined that preserved Nummulites suggest the deposition in proximal parts of fore-reef. This specific facies is interpreted to be formed on proximal parts of fore-reef in high-energy conditions.

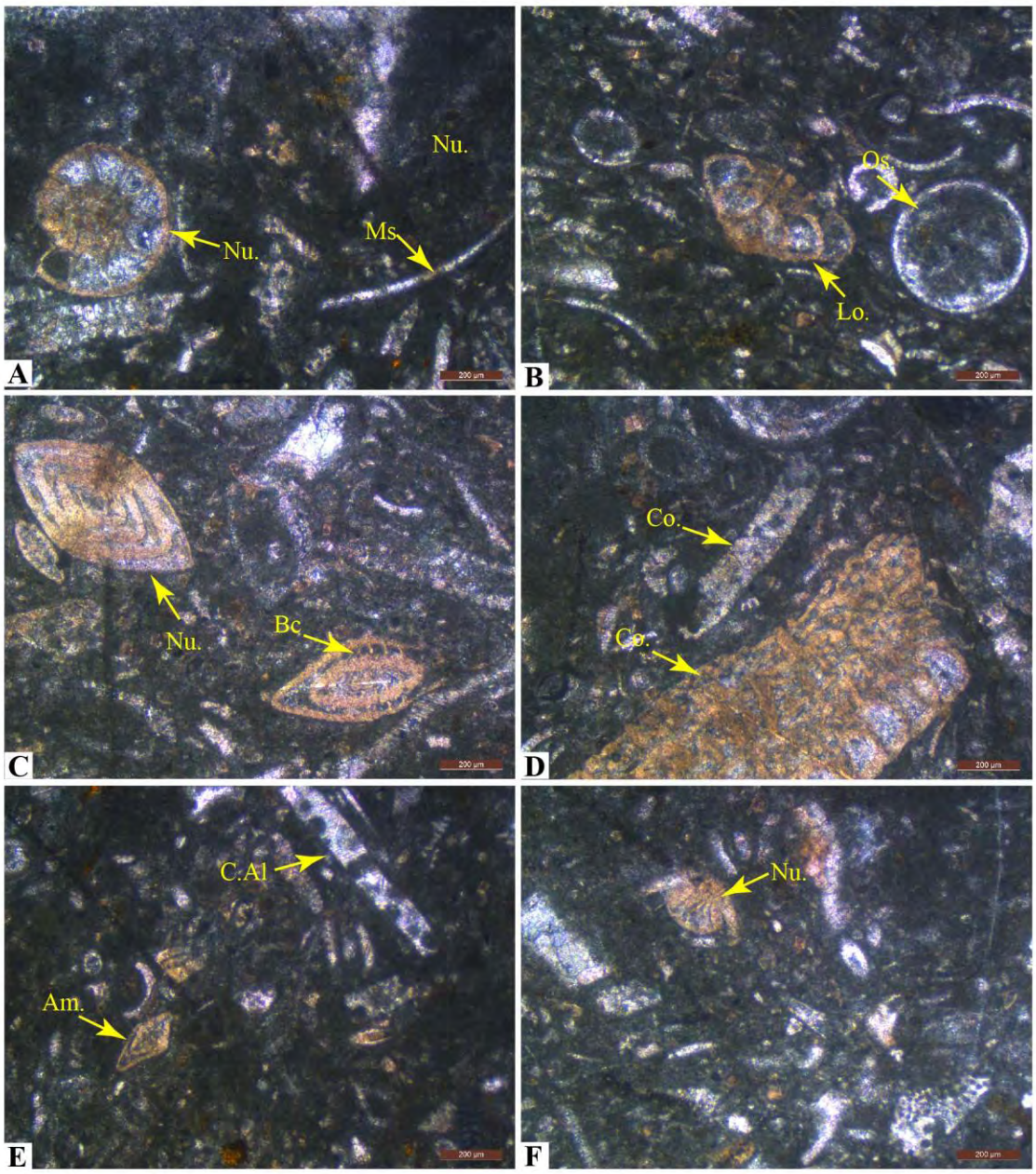

Figure 5.12: Coralline Nummulitic Bioclast Packstone (MF12). Nu.= Nummulite sp., Ms= Mullascan sp., Os.= Ostracod shell, Lo= Lockartia sp., C.Al= calcareous algae, Amphistegina

5.2 Diagenesis

The term diagenesis describes the chemical and physical events that have an impact on sedimentary rocks after their deposition and right before their metamorphism. Micritization, dehydration, bioturbation, cementation, dissolution, fracturing, compaction, dolomitization, and pyritization are some of the most substantial changes carried out by diagenesis (Tucker, 2007). The textures that developed during deposition were altered and eradicated by diagenesis, which also produced a new secondary texture and increased the reservoir potential by fracturing (Croizé et al., 2010).

5.2.1 Micritization: Micritization is the early stage of diagenesis and micrites were formed around the alochems due to the microbial activity. In Figure 5.13A micritization is shown around the nummulitic species. Micritization occurs mostly in the shallow marine environment where microorganisms are found that cause this specific diagenetic event (Reid & MacIntyre, 2000; Beigi et al., 2017). It is influenced by the rate of the deposition of sediments and water depth. In Drug Formation, micritization can be seen in various thin sections.

5.2.2 Bioturbation: Bioturbation is depicted by burrows, is the alteration of sediments by organisms that ruins the texture. It occurs most frequently in low-energy marine phreatic environments (Flügel, 2010). Bioturbation is characteristic of the shallow marine environment but can be found in deep marine and can be seen in Figure 5.13 B & C.

5.2.3 Dissolution: Dissolution took place in carbonate rocks by weak acids as the carbonate matrix is highly dissolvable. When the pore fluids are less saturated with the carbonate minerals it results in the dissolution of the carbonate matrix and forms secondary porosity. Figure 5.13 D shows the cavities formed by the dissolution and part of it is filled by the calcite cement.

5.2.4 Blocky calcite cement: The formation of blocky calcite in the void spaces is also another evidence of diagenesis. It occurs when the pore fluids are supersaturated with the calcites then these calcites start to precipitate into the void spaces and reduce the porosity of the rock. It formed in low-energy environments. Figure 5.13 E & F shows the blocky calcite filling the void spaces.

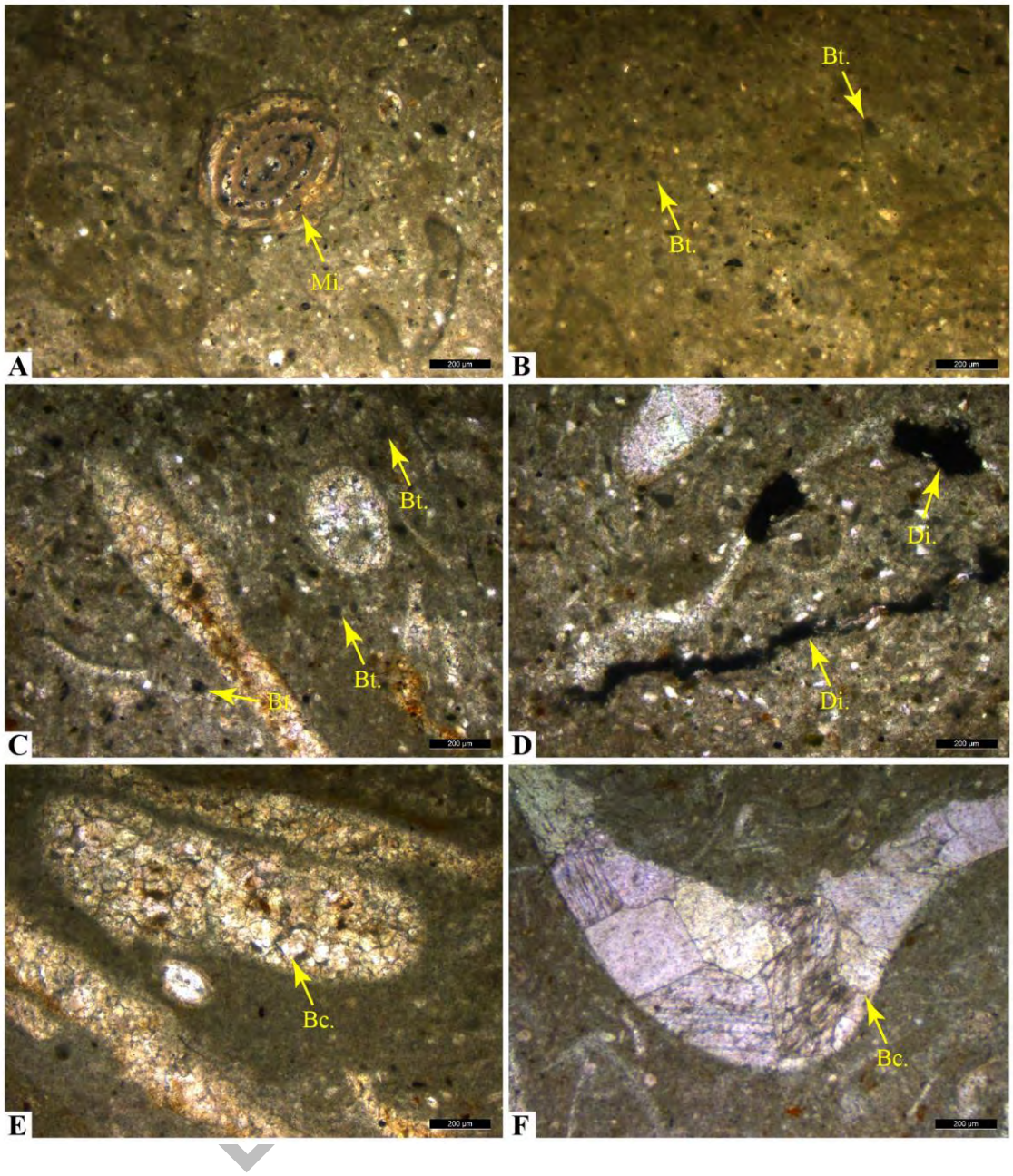

Figure 5.13: Diagenesis of Drug Formation. A. Micritization along the edges of nummulite sp., B&C Bioturbation by micro-organisms, D. Void spaces created by dissolutions, E&F. Blocky calcite cementation. Mi.= Micritization, Bt.= Bioturation, Di.= Dissolution, Bc.= blocky calcite.

5.2.5 Chemical and mechanical compaction: Compaction occurs due to pressure solution (Lloyd, 1977) and physical pressure (Shinn & Robbin, 1983) respectively. Physical compaction is due to the overburden of newly deposited sediments which put pressure on the underlain sediments and results in the dehydration and rearrangement of sediments and causes compaction. If chemical and mechanical compaction occurs at the same time it reduces the volume of the rock significantly. In figure 5.14 A & B compaction is shown.

5.2.6 Dolomitization: It is a process where calcium in calcites is replaced by magnesium, which results in the formation of dolomite also changing the crystal structure and volume of the rock. Magnesium ion is smaller than the calcium ion so after the replacement volume of the rock reduces which also increases the porosity of the rock (Weyl, 1960). In figure 5.14 B & C dolomitization is shown in some of the studied samples.

5.2.7 Fracturing: Rock characteristics and pore pressure can be gradually changed via diagenesis, which will impact the formation of fractures in the rock (Laubach et al., 2009). In fractures, precipitation and dissolution can harden, enlarge, or close the fracture. In figure 5.14 C fracturing in the samples of Drug Formation is shown.

5.2.8 Transparent calcite: Transparent calcite deposited in the fractures and voids spaces formed into the rock during diagenesis when fluids saturated with calcites run through it pure calcite crystallized into the spaces appearing transparent (Figure 5.14 E & F).

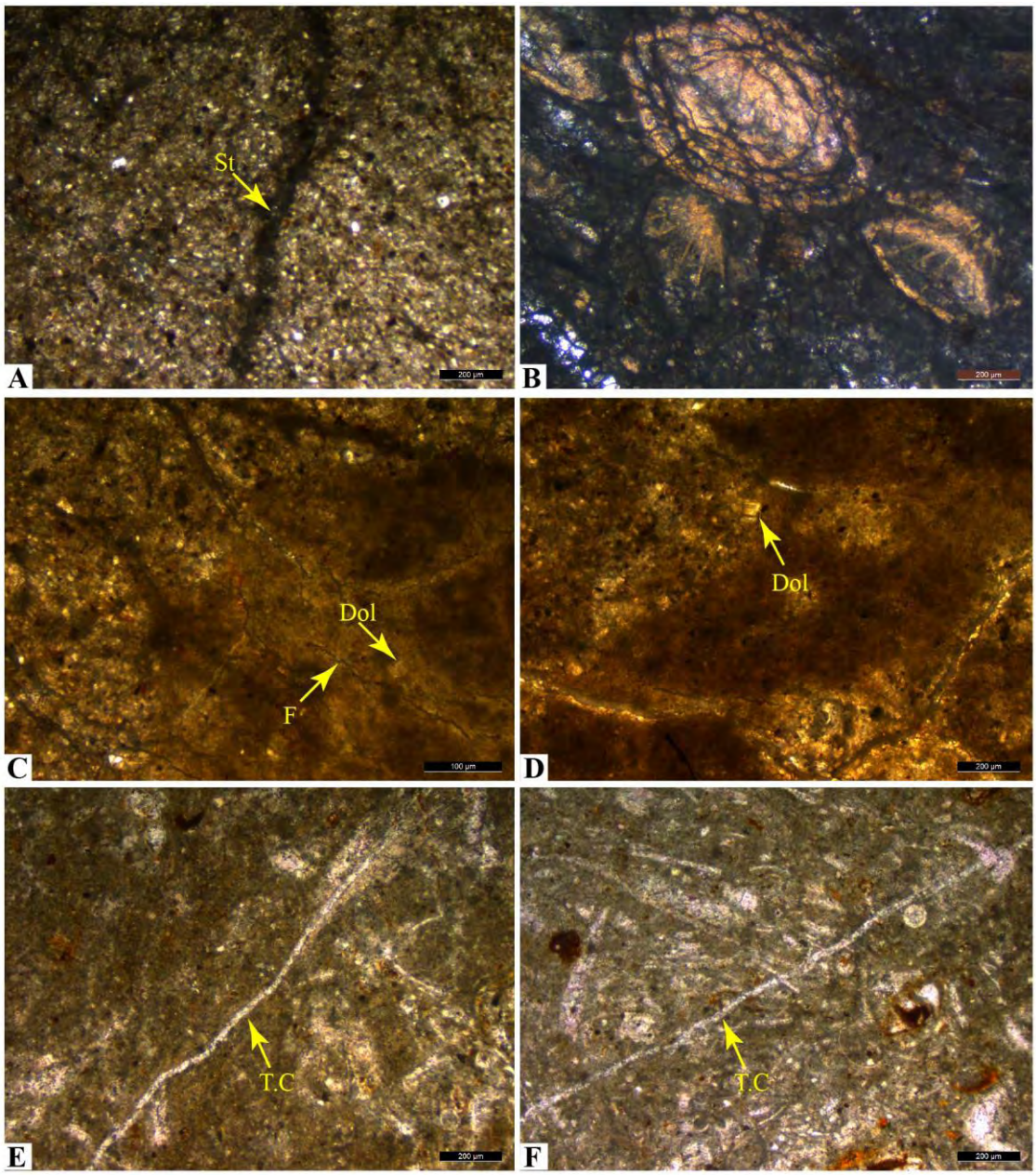

Figure 5.14: Diagenetic Phases of Drug Formation. A. Chemical Compation identified by the presence of stylolites, B. Physical Compaction identified by distortion in nummulites, C. Dolomitization and Fracturing, D. Dolomitization, E&F. Telogentic calcite. St.= Stylolites, Dol.= dolomitic rhomb, F= Fracture, T.C= Telogenetic calcite

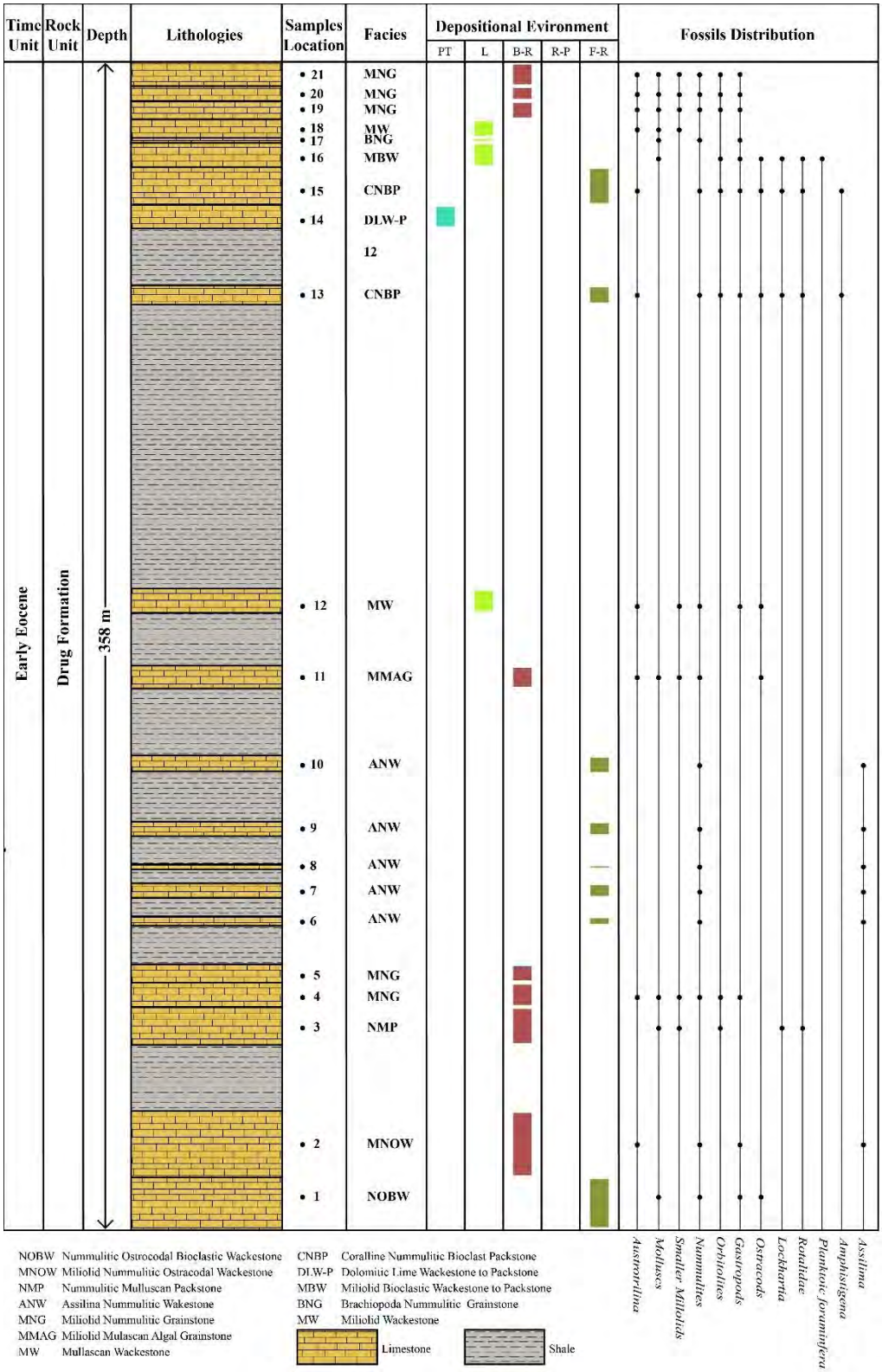

Figure 5.15: Detailed Log of Drug Formation, showing Lithologies, Sample Locations, Micrfacies, Depositionl Environment and Biota Distribution.,

5.3 Depositional Environment

The investigation of microfacies analysis unravel total twelve microfacies grouped into four classes based on the same depositional settings, that is tidal, lagoonal, back-reef and fore-reef facies. The tidal facies includes only MF1, lagoonal facies includes MF2-5, back-reef facies are MF6-9 and fore reef facies are MF10-12. While no middle outer shelf facies are recorded signify to inner shelf environment.

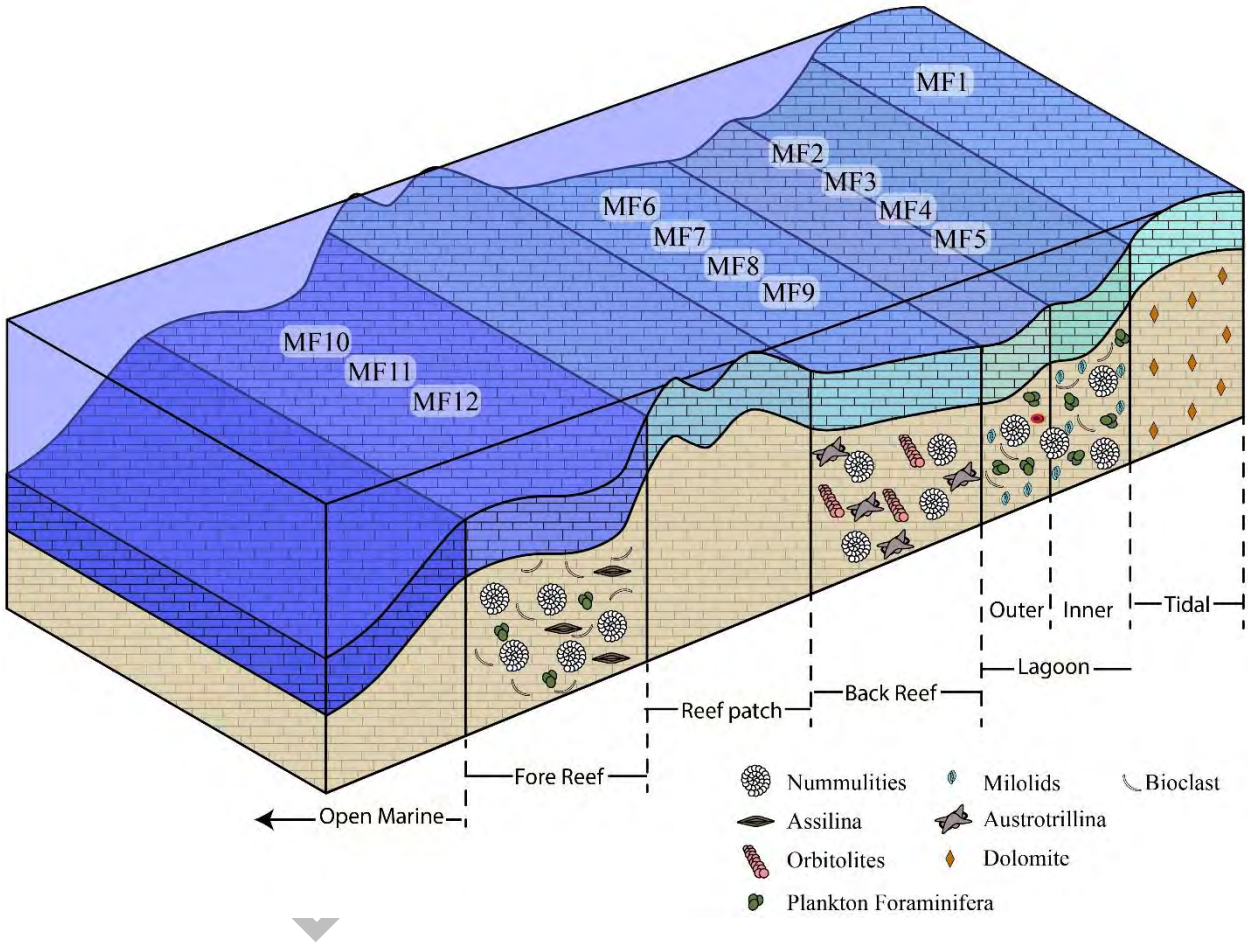

Figure 5.16: Depositional Model of Drug Formation.

5.4 Paragenetic Sequence

The Drug Formation's comprehensive paragenetic sequence has been documented based on field observations, petrography results, and geochemical investigation (Figure 5.15). A petrographic study revealed that early to late-stage diagenesis took place in Drug Formation.

A. The original depositional texture underwent considerable alteration during the eogenetic phase of diagenesis (early stage of diagenesis) as a result of substantial micritization. Micritization is a property of shallow marine phreatic zone diagenesis where microorganisms got adequate time for the process. These organisms dig through

the sediments destroying the further texture of sedimentary rock in the shape of burrows, which is significant in shallow marine and less significant in deeper marine settings.

B. Dissolution is where bioclastic remnants and carbonate grain dissolve into the less saturated fluids during marine to meteoric phreatic zone.

C. Blocky calcites started to deposit into the pore spaces from supersaturated fluids during a meteoric phreatic zone to the initial burial stage, reducing the porosity of the rock.

D. Burial in the mesogenetic stage causes the compaction of sediments. The mechanical compaction brought about by the overlaying layers of sediments and the development of macro and micro fractures. Chemical compaction gives rise to suture seams and stylolites.

E. Dolomitization appears in the late stage of burial, mostly along the fractures due to the fluids.

F. Fracturing occurs from late stage mesogenetic zone to early telogenetic zone. Burial cause fracture due to the overburden pressure as well as uplift also caused multiple fractures.

G. Deposition of transparent calcite forming the calcite veins is a feature of telogenetic diagenesis.

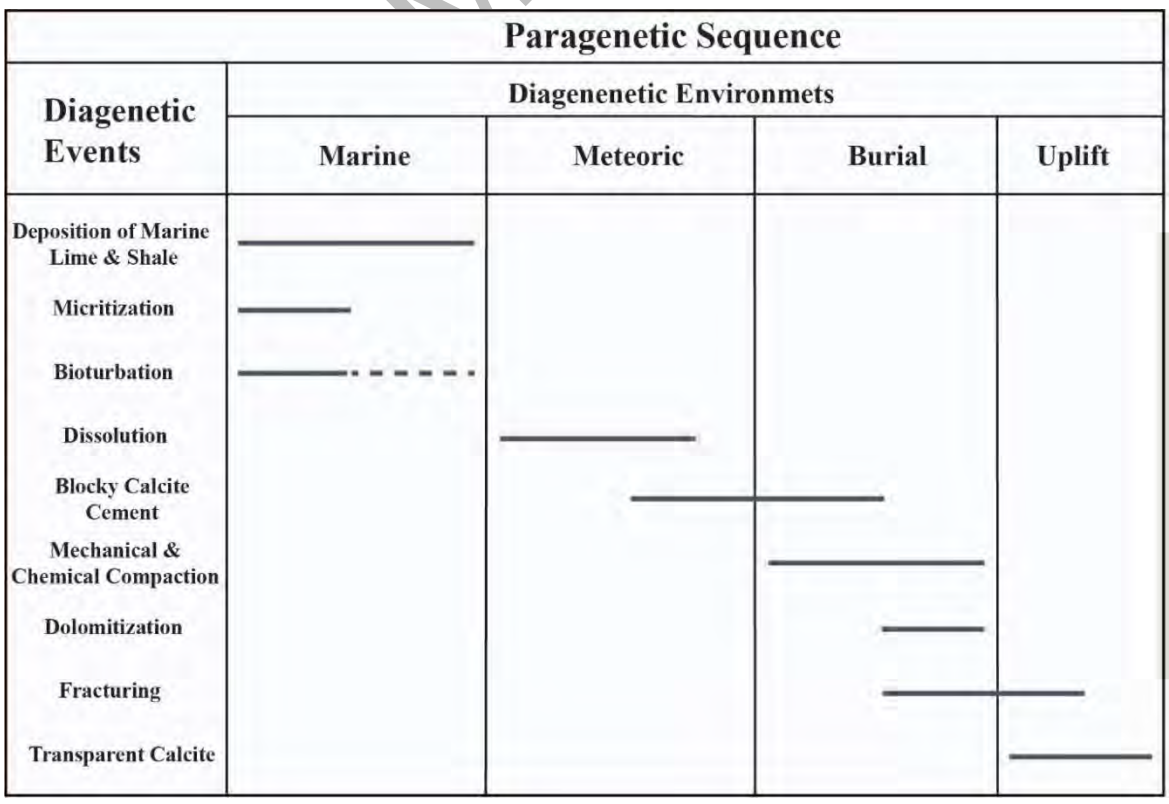

Figure 5.17: Paragenetic sequence of Drug Formation.

CHAPTER 6

Source Rock and Reservoir Characterization

6.1 Source Rock

The raw material for the formation of hydrocarbons is distributed organic material in sediments, and the amount of presence of organic matter is a major aspect in assessing the potential for the generation of hydrocarbons (Hunt 1995).

The right evaluation of the hydrocarbon potential and the geochemistry of the source rock is made possible by the quantity, quality, and thermal maturation of the organic matter. The collected data by pyrolysis of the study area are placed against each other in cross plots or scatter plots employed to analyze the characteristics and hydrocarbon potential. The TOC, free hydrocarbon (S_1), pyrolyzed hydrocarbon (S_2), amount of CO_2 (S_3), and temperature at which the highest amount of the pyrolysis products generated (T_{max}) are used to determine the production index (PI), genetic potential (GP), oxygen index (OI), and hydrogen index (HI) according to the following formulas:

$$\text{Genetic Potential (GP)} = S_1 + S_2$$

$$\text{Production Index (PI)} = \frac{(S1 + S2)}{S1}$$

$$\text{Oxygen Index (OI)} = 100 \times \frac{S3}{TOC}$$

$$\text{Hydrogen Index (HI)} = 100 \times \frac{S2}{TOC}$$

TOC results and rock-eval pyrolysis data are shown in table 6.1.

Table 6.1: Rock-Eval analysis of Drug Formation

Depth (ft)	**TOC** (wt %)	**S1** (mg/g rock)	**S2** (mg/g rock)	**S3** (mg/g rock)	**T max**	**GP** (mg/g rock)	**PI**	**OI**	**HI**
0	1.50	0.27	1.72	0.84	421	1.99	0.13568	56	114.667
0	1.90	0.32	2.5	0.61	438	2.82	0.11348	32.1053	131.579
0	1.63	0.53	0.53	0.54	425	1.06	0.5	33.1288	32.5153
0	1.45	0.38	0.38	0.56	417	0.76	0.5	38.6207	26.2069

6.1.1 Organic Kerogen Environment

It is the environment where organic material from plant residue or from organisms is estimated to be preserved. The organic environment can be revealed through the graph between oxygen index (OI) and hydrogen index (HI). In figure 6.1, the graph of kerogen environment taking the oxygen index on x-axis and hydrogen index on y-axis, the data is plotted between the anoxic environment and terrestrial environment showing the kerogen environment as a transition between two environments, anoxic and terrestrial, environment having enough hydrogen but lacks oxygen.

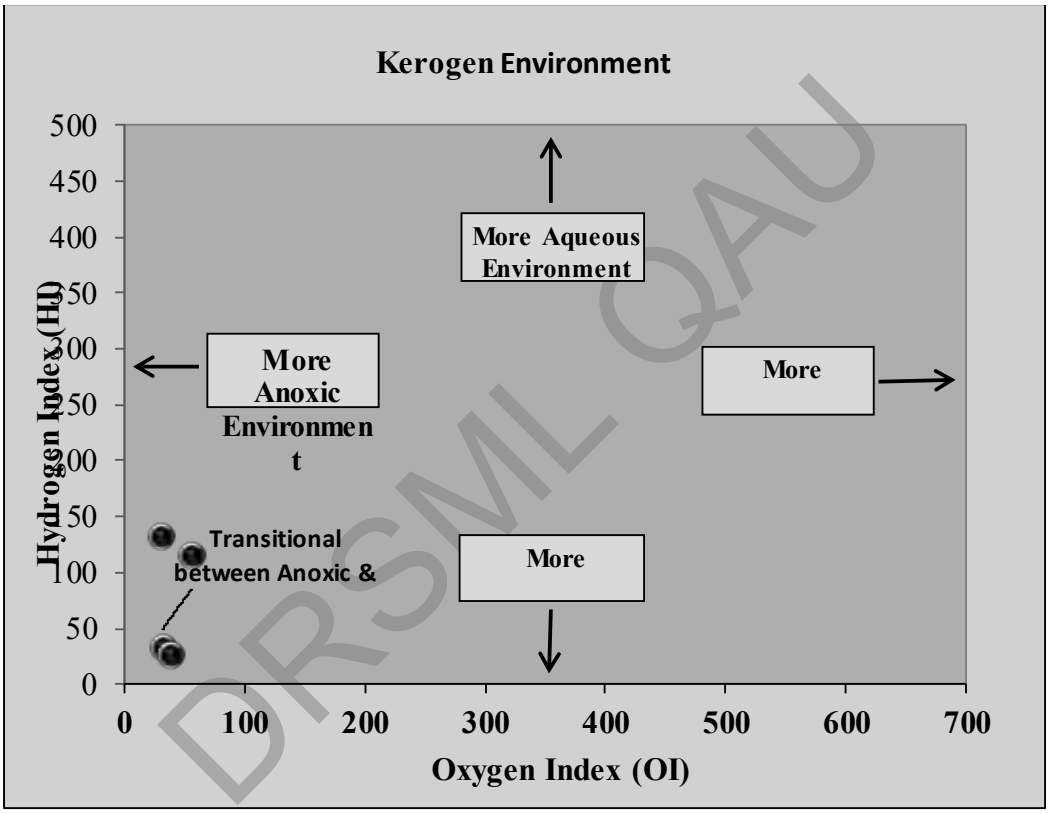

Figure 6.1: Kerogen Environment of the study samples.

Kerogen Type and Maturation

The nature of organic material has a consequential role in determining the hydrocarbon products' type and is an essential factor while assessing source rock potential. Since organic materials and hydrocarbons vary in their chemical makeup, it is essential to distinguish the different kerogen forms. In Figure 6.2 show the kerogen type of the studied samples, which leans more towards the Kerogen type-III. The nature of organic content is a crucial factor in determining the capability of source rocks and has an impact on the type of hydrocarbon

product. Sedimentary rocks include four different forms of kerogen, as per Peters & Cassa (1994) and Jacobson (1991).

Type-I It is comprised of oil-forming hydrogen material, from certain marine sediments in lacustrine deposits.

Type-II Similarly made up of organic materials rich in hydrogen and likely to produce oil in marine sediments, despite the fact that oil is Type-II kerogen's primary product but generates more gas than kerogen Type-III (Hunt, 1995).

Type-III Consisting primarily of terrestrial wood base plant material with less hydrogen in it producing gas as its main product.

Type-IV It is made of passive and inactive carbon that has minimal to no producing potential.

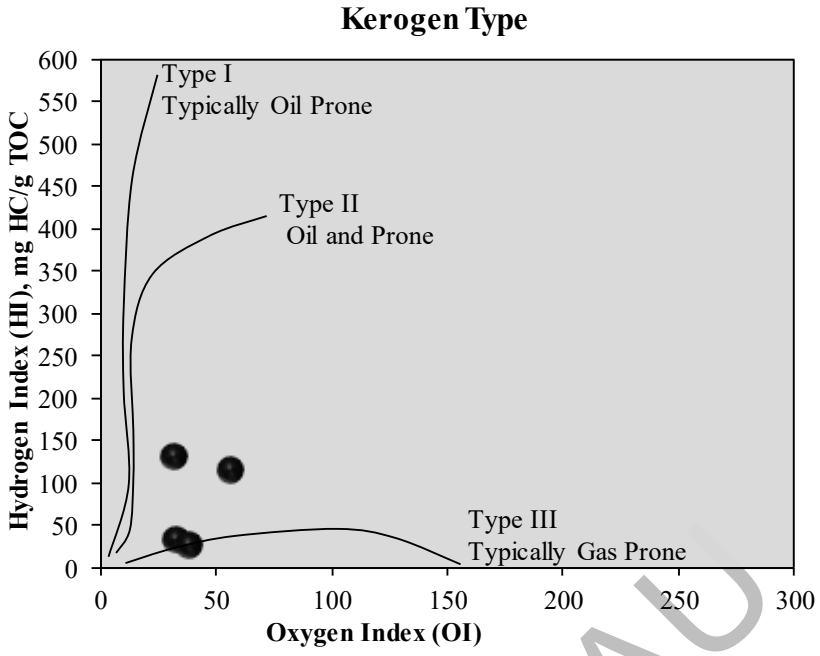

Figure 6.2: Kerogen type of the studied samples.

Quality and maturity of kerogen was evaluated by graphing HI versus T_{max}. HI and T_{max} of the studied sample are plotted in figure 6.3.

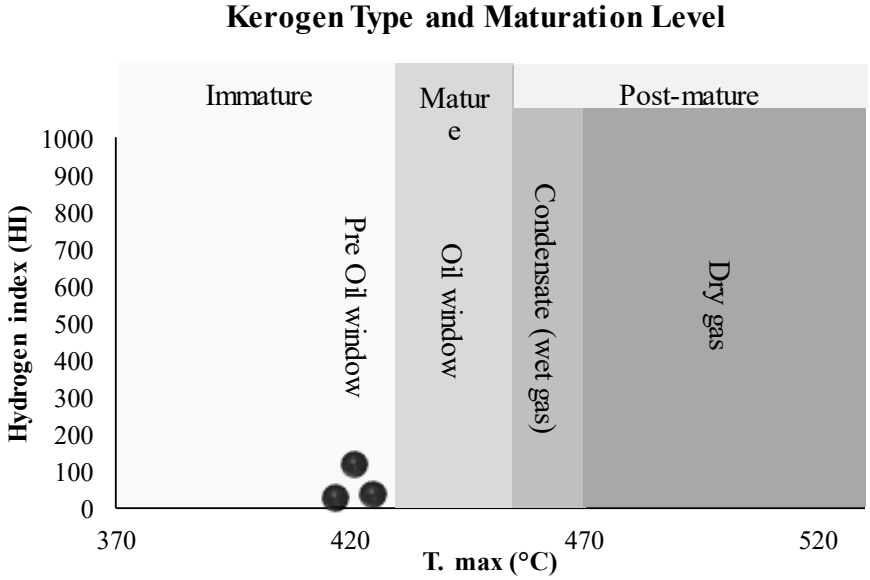

Figure 6.3: Kerogen Quality and Maturation Level of studied Samples.

Quality of Source Rock

Welte & Tissot (1984) suggested genetic potential (GP) to classify source rocks through which source rocks were classified into three categories good, moderate, and poor. Rock with genetic potential less than 2mg/g is considered a poor source rock and is gas potential, if GP is in-between 2 and 6mg/g the rock is considered to be a moderate source rock with medium gas and oil potential, Having genetic potential more than 6 is good quality source rocks and are oil-prone. A figure of classification of the studied sample on the basis of genetic potential is given in figure 6.4. Which tells that source rock quality of Drug Formation lies between fair to poor.

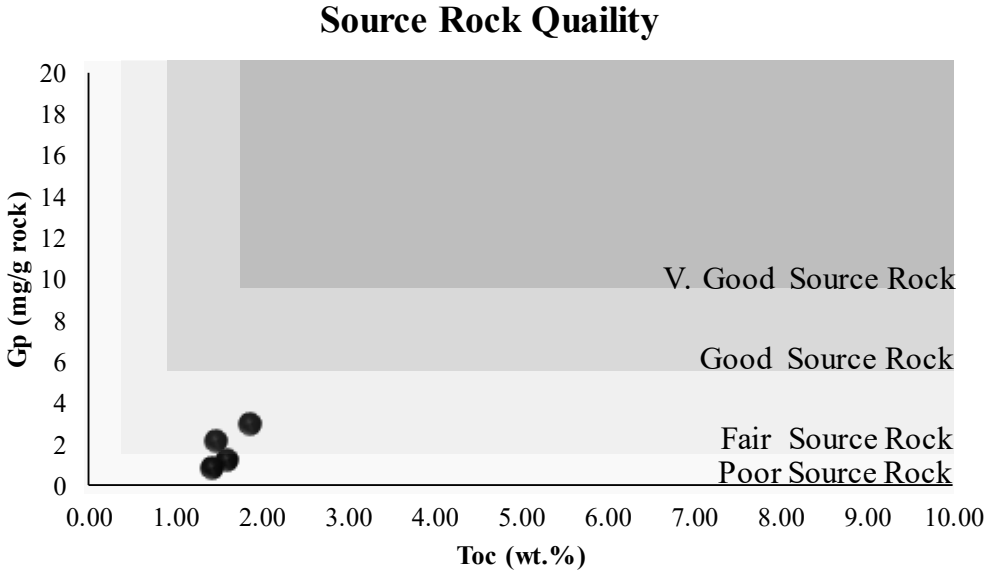

Figure 6.4: Source rock quality Classification of studied samples.

Maturity

Maturity is the level of heating-induced thermal change in organic material (Peters & Cassa, 1994). Carbonate rock that is subjected to enough pressure for diagenesis but hasn't visibly been impacted by temperature is said to be immature, it is subjected to a temperature less than 435°C. Mature source rock has gone through enough pressure and temperature 435-450°C while post-mature hydrocarbon produces gas because it lacks hydrogen owing to the impact of high temperatures >450°C. The graph of source rock maturity plotted between the production index (x-axis) and depth (y-axis) is given in figure 6.5. Drug Formation is more of an immature source rock.

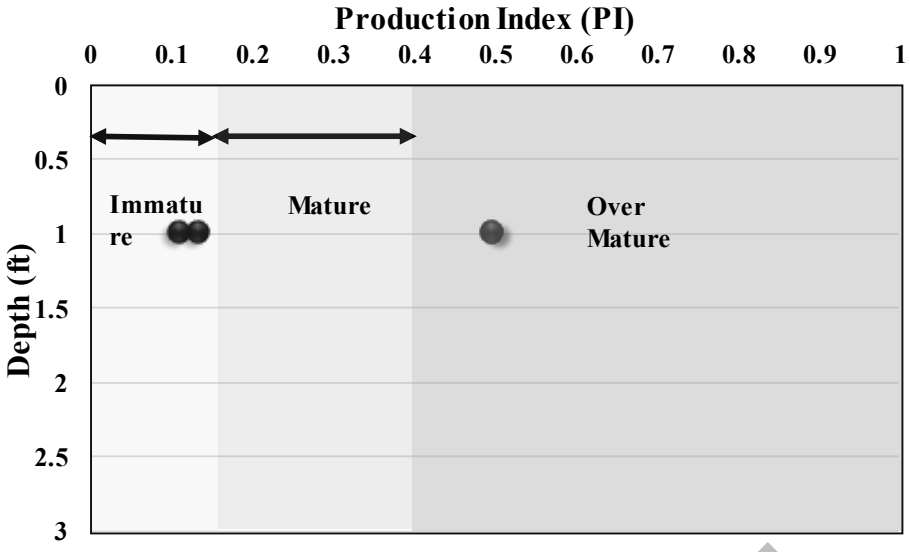

Figure 6.5: Maturity of Studied Samples.

Indigenous and Non-Indigenous Hydrocarbons

Indigenous hydrocarbons are those that are not migrated after production while non-indigenous hydrocarbons are hydrocarbons that got migrated from their original place. To find the non-indigenous and indigenous hydrocarbons a graph is plotted between free hydrocarbons and total organic carbon in figure 6.6.

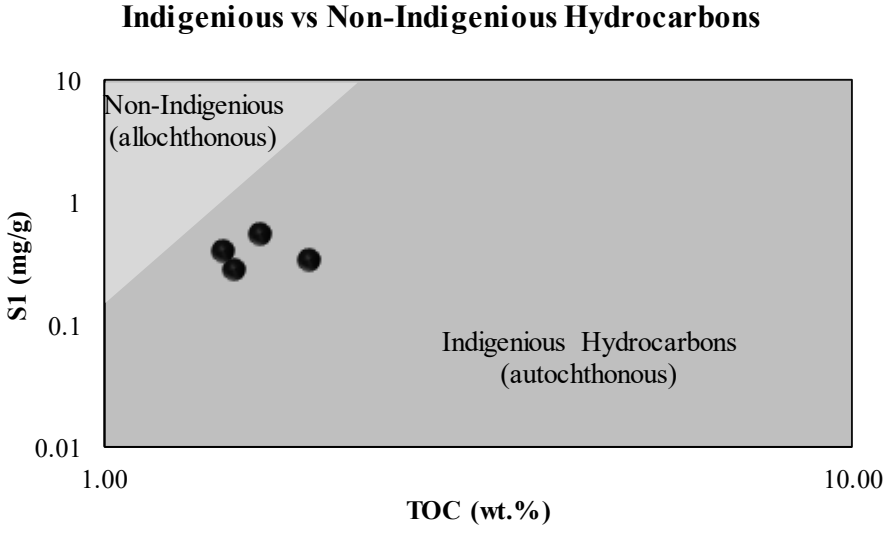

Figure 6.6: Indigenous and non-indigenous graph between S1 and TOC.

Type of organic matter/ Quantity of Source Rock

The richness of organic materials and the potential for the production of hydrocarbons were assessed using TOC. On the base of TOC, it is a good quality source rock.

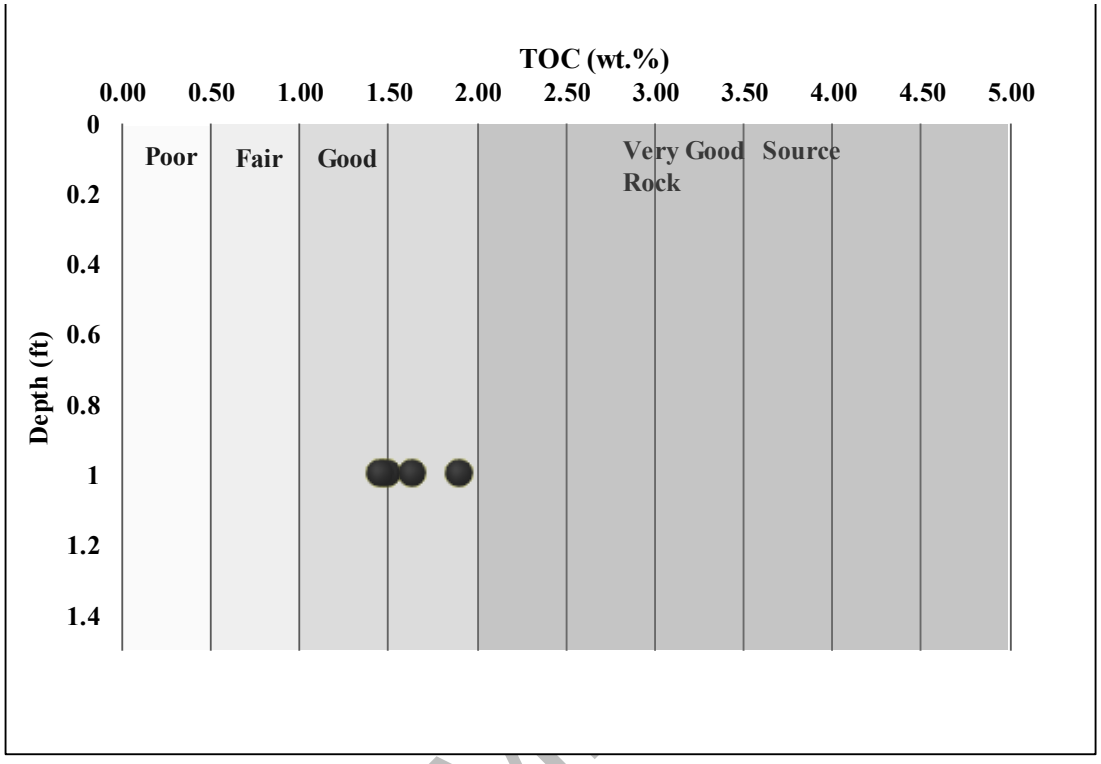

Figure 6.7: Type of Organic matter.

Source rock potential

The graph between genetic potential and depth tells us the potential of the source rock.

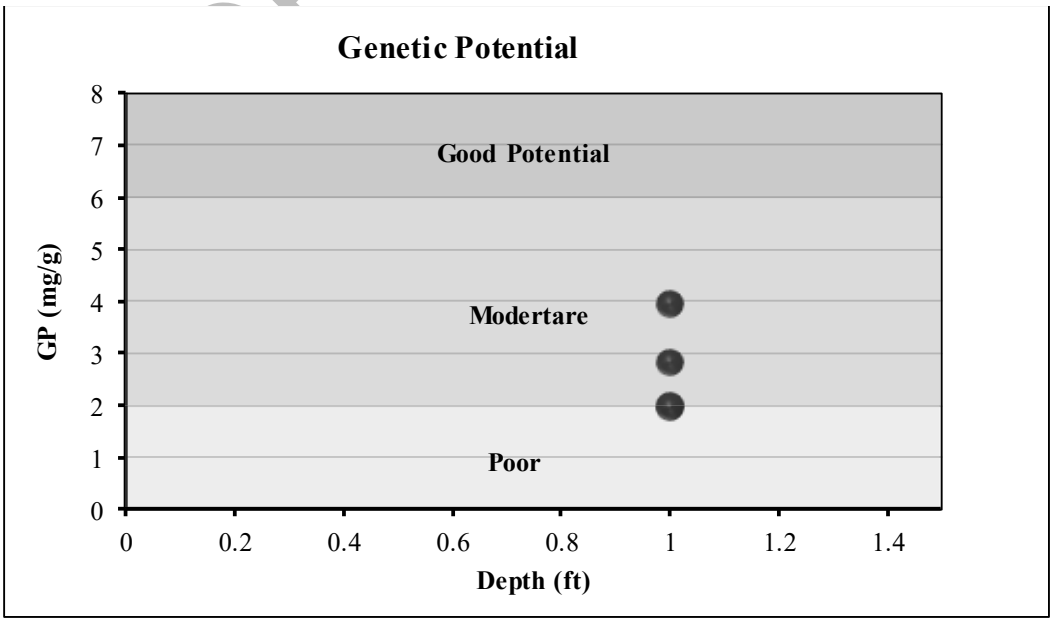

Figure 6.8: Source Rock potential of Drug Formation.

Reservoir Quality Parameters

The ability to withhold fluids and transportation is considered a reservoir quality. The porosity and permeability of a rock affect the quality of the reservoir. But both of these are frequently challenging to anticipate because they are dependent on depositional environments and diageneses (Amjad et al., 2023). Reservoir quality measures like the reservoir quality index and the Flow zone indicator were first proposed by Amaefule et al. in 1993.

Four samples of Drug Formation were run to find the air permeability and air porosity. Air permeability and air porosity of Millolid Wakestone is 0.31 and 7.48 respectively. For Dolomitic Lime Wake to Packstone air permeability and porosity is 0.14 and 6.17 respectively. Air permeability for Nummulitic Mullascan Packstone is 0.03 and air porosity is 3.53 while air permeability for Millolid Nummulitic Grainstone is 0.02 and porosity is 1.73 (Table 6.2).

	Air Permeability	**Air Porosity**
MW	0.31	7.48
DLW-P	0.14	6.17
NMP	0.03	3.35
MNG	0.02	1.73

Table 6.2: Air permeability and air porosity of tested samples. Where MW = Millolid Wakestone, DLW-P = Dolomitic Lime Wake to Packstone, NMP = Nummulitic Mullascan Packstone, and MNG = Millolid Nummulitic Grainstone

The bar graph between the air permeability and air porosity mentioned in the above table is shown below in figure 6.9.

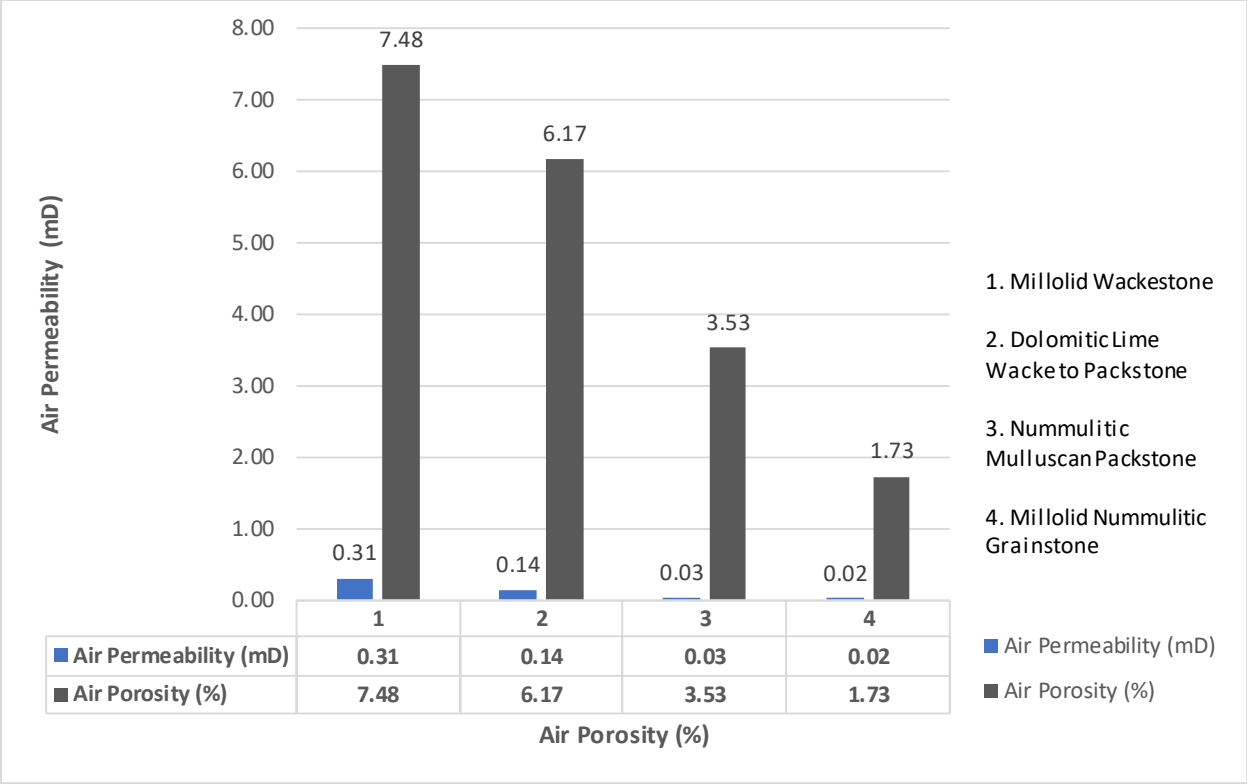

Figure 6.9: Bar Graph of Permeability and Porosity.

ØHe (Helium Porosity) is just Air porosity in decimals. Normal porosity Øz can be found by dividing ØHe with 1- ØHe. The Reservoir quality index (RQI) and flow zone indicator (FZI) are calculated through the following formulas:

$$Øz = \frac{ØHe}{1-ØHe}$$

$$RQI = 0.0315\sqrt{\frac{k}{ØHe}}$$

$$FZI = \frac{RQI}{Øz}$$

Where k is permeability in md, ØHe is helium porosity in decimals and Øz is normal porosity in decimals while RQI and FZI are measured in µm.

Table 6.3: Porosity, Permeability, and reservoir Quality properties of the studied samples.

Air Permeability K (md)	Air Porosity ØHe (%)	ØHe decimal	Øz (dec)	RQI	FZI
0.31	7.48	0.0748	0.0845	0.06014	0.71172
0.14	6.17	0.0617	0.065	0.046	0.70769
0.03	3.53	0.0353	0.03018	0.02904	0.96219
0.02	1.73	0.0173	0.0559	0.018	0.322

Reservoirs ranked on the base of porosity, permeability, reservoir quality index, flow zone indicator, and reservoir potential index. When a reservoir has a porosity greater than 25% and permeability greater than 1000md with a reservoir quality index of 5.00µm, Flow zone indicator greater than 15, and reservoir potential index of excellent can rank the reservoir rock at number 1. Reservoir rock has a porosity of 20 to 25%, permeability between 100 to 1000md with a reservoir quality index of 2.00 to 5.00 µm, Flow zone indicator of 10.0 to 15 µm, and reservoir potential index of very good then reservoir rock's rank will be number 2. If porosity ranges from 15 to 20%, permeability ranges between 10 to 100md with a reservoir quality index of 1.00 to 2.00 µm, Flow zone indicator 5 to 10 µm, and reservoir potential index is good then rank of the reservoir rock will be number 3. Porosity ranging from 10 to 15%, permeability from 0.1 to 10md with reservoir quality index 1.00 to 2.00 µm, Flow zone indicator 2.50 to 5 µm, and fair reservoir potential index then reservoir rock rank at number 4. If porosity ranges from 5 to 15%, permeability ranges between 0.10 to 10md with reservoir quality index 0.25 to 1.00 µm, Flow zone indicator 0.25 to 5 µm then reservoir potential index will be poor and reservoir rock ranked at 5. When a reservoir rock has a porosity of 5% or 0 and permeability of 0 or equal to 0.1md with a reservoir quality index of 0 to 0.25µm, Flow zone indicator 0 to 1.00 µm then the reservoir potential index will say to be tight, and ranking the reservoir rock at number 6.

On the base of reservoir quality parameters, Millolid Wakestone and Dolomitic lime Wake-Packstone lies in poor reservoir potential index with reservoir rock ranked at number 5 while Millolid Nummulitic GRainstone and Nummulitic Mullascan Packstone demonstrate a tight reservoir potential index, ranking on number 6 in reservoir rock.

In Figure 6.10 graph between the flow zone indicator and reservoir quality index is shown. Representing the reservoir potential.

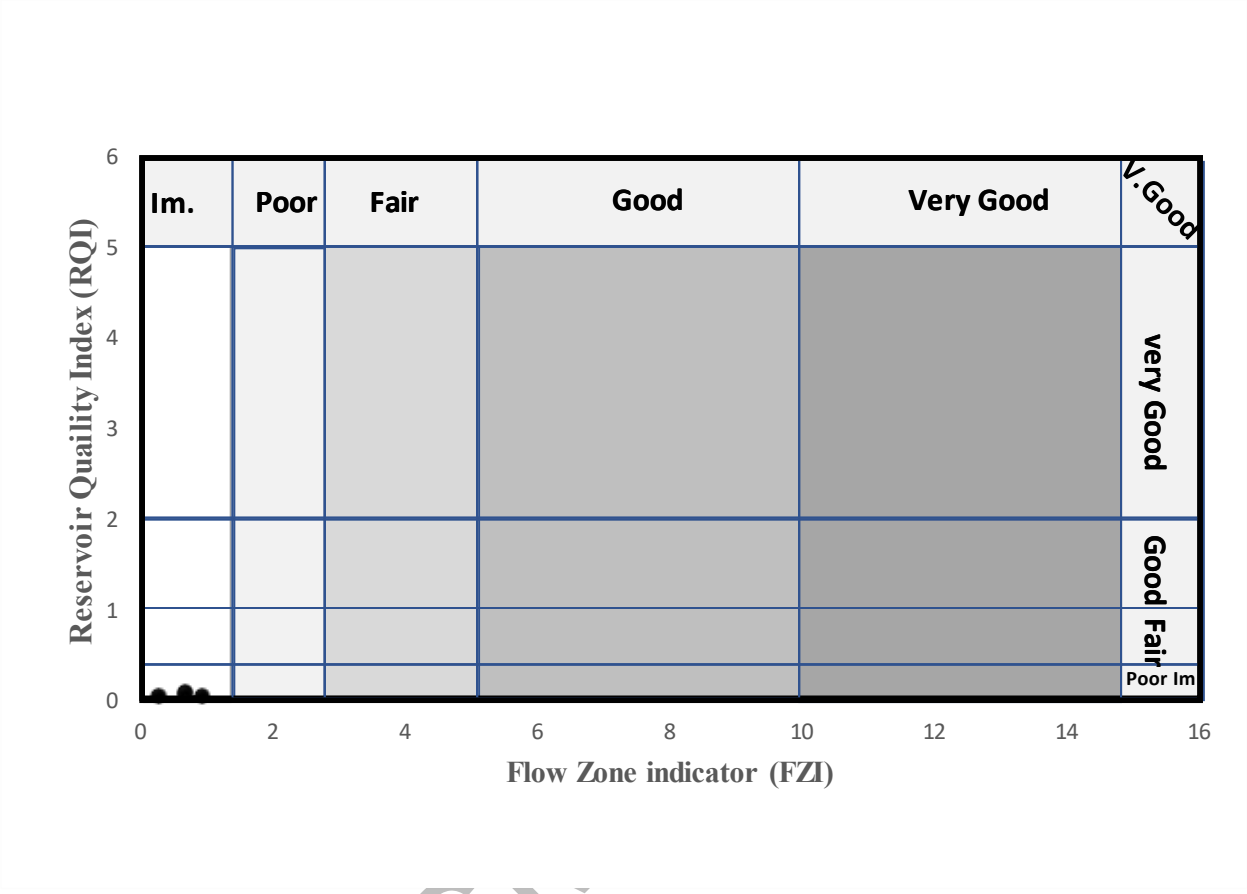

Figure 6.10: Reservoir potential of Drug Formation

Reservoir potential index of the Drug Formation base on the plug analysis of studied samples lies in the immature reservoir quality.

CHAPTER 7

Discussions and conclusions

- Drug Formation in the Zindapir Anticline section is comprised of limestone with intercalated shale beds. Limestone is off-white/yellow to grey in color, while shales are green to grey in color. The formation is thickly bedded in the lower area. The Drug Formation has a definite bottom contact with the Shaheed Ghat Formation and a upper contact with the Baska Formation. Its total measured thickness in the field is 358m.
- In the lower unit Drug Formation have massive shale beds and the upper unit is comprised of mostly limestone beds having little to no intercalated shales observed in the field.
- Microfacies analysis of Drug Formation tells the formation is deposited in the inner-shelf environments: tidal, lagoonal, back-reef, and fore-reef.
- The tidal-flat environment facie consists of fine crystalline dolomite in lime muddy matrix.
- Lagoonal environment facies have milliolids, amphistegina, austrotrillina, inarticulated and articulated mullascan shells, nummulitic sp., and planktic foraminifera deposited in muddy inner platforms.
- Back-reef facies comprised of nummulitic sp. with milliolids, ostracodal & mullascan assemblage, austrotrilina, orbitolite fragments, and some gastropod shell remains deposited in low energy environments of the inner shelf.
- Fore-reef facies of the inner shelf consist of bioclast that contains ostracodal fragments, gastropod remains, nummulitic sp., amphistegina, coralline algae and some assilina.
- Drug Formation has gone through significant changes because of diagenesis: micritization, bioturbation, dissolution, crystallization of blocky calcite cement, compaction, dolomitization, fracturing, and transparent calcite veins.
- Marine diagenesis of Drug Formation includes micritization around the allochems and bioturbation is significant in shallow marine and less significant in deeper settings of marine environments.
- The meteoric diagenesis phase shows the phenomenon of dissolution giving rise to secondary porosity and crystallization of blocky calcite cement in pore spaces.
- Mechanical and chemical compaction takes place in burial diagenesis resulting in dolomitization along the vein fillings.

- During telogenesis fracturing and calcite, vein filling takes place while the rocks were subjected to tectonic uplift.
- Source rock characterization of studied samples showed Drug Formation is fair to good source rock with an immature production index.
- The plug analysis showed that the depositional texture of Drug Formation is impervious and of poor reservoir quality.

References

Abd El-Moghny, M. W., & Afifi, A. A. (2022). Microfacies analysis and depositional environments of the Middle Eocene (Bartonian) Qurn Formation along Qattamiya—Ain Sokhna district, Egypt. *Carbonates and Evaporites*, *37*(1), p 18.

Abdel-Gawad, M. (1971). Wrench movements in the Baluchistan arc and relation to Himalayan-Indian Ocean tectonics. *Geological Society of America Bulletin*, *82*(5), 1235-1250.

Ahmad, S., Wadood, B., Khan, S., Ullah, A., Mustafa, G., Hanif, M., & Ullah, H. (2020). The sedimentological and stratigraphical analysis of the Paleocene to Early Eocene Dungan Formation, Kirthar Fold and Thrust Belt, Pakistan: implications for reservoir potential. *Journal of Sedimentary Environments*, *5*(4), 473-492.

Al Moqbel, A., & Wang, Y. (2011). Carbonate reservoir characterization with lithofacies clustering and porosity prediction. *Journal of Geophysics and Engineering*, *8*(4), 592-598.

Amaefule, J., Altunbay, M., Tiab, D., Kersey, D., Keelan, D., 1993. Enhanced reservoir description using core and log data to identify hydraulic flow units and predict permeability in uncored intervals/wells. SPE 26436, 205–220. https://doi.org/10.2118/26436-MS.

Amjad, M. R., Ehsan, M., Hussain, M., Al-Ansari, N., Rehman, A., Naseer, Z., ... & Elbeltagi, A. (2023). Carbonate Reservoir Quality Variations in Basins with a Variable Sediment Influx: A Case Study from the Balkassar Oil Field, Potwar, Pakistan. *ACS Omega*.

Babazadeh, S. A., & Alavi, M. (2013). Paleoenvironmental model for Early Eocene larger benthic foraminiferal deposits from south Birjand region, east Iran. *Revue de Paléobiologie, Genève*, *32*(1), 223-233.

Bannert, D., Iqbal M., Helmcke D. (1995). Surface and Subsurface evidence for the existence of the Sulaiman Basement fault of the north-western Indian plate in Pakistan. In Abstract, South Asian Geological Congress, Colombo, Sri Lanka, p21.

Bassi, D., & Nebelsick, J. H. (2010). Components, facies and ramps: redefining Upper Oligocene shallow water carbonates using coralline red algae and larger foraminifera

(Venetian area, northeast Italy). *Palaeogeography, Palaeoclimatology, Palaeoecology*, *295*(1-2), 258-280.

Beigi, M., Jafarian, A., Javanbakht, M., Wanas, H.A., Mattern, F. and Tabatabaei, A., 2017. Facies analysis, diagenesis and sequence stratigraphy of the carbonate-evaporite succession of the Upper Jurassic Surmeh Formation: Impacts on reservoir quality (Salman Oil Field, Persian Gulf, Iran). Journal of African Earth Sciences, 129, pp.179-194.

BouDagher-Fadel, M. K., & Wilson, M. (2000). A revision of some larger foraminifer of the Miocene of southeast Kalimantan. *Micropaleontology*, *46*(2), 153-165.

Boudaugher-Fadel, M. K. (2018). *Evolution and geological significance of larger benthic foraminifera*. UCL press.

Brasier, M. D. (1975). The ecology and distribution of recent foraminifera from the reefs and shoals around Barbuda, West Indies. *The Journal of Foraminiferal Research*, *5*(3), p 193-210.

Burchette, T. P., & Wright, V. P. (1992). Carbonate ramp depositional systems. *Sedimentary geology*, *79*(1-4), 3-57.

Carozzi, A. V. (1988). Carbonate rock depositional models: A microfacies approach. Englewood Clifs: Prentice Hall

Chapter 2: Facies analysis - magellan.kgs.ku.edu. (n.d.). Retrieved November 28, 2022, from https://magellan.kgs.ku.edu/PRS/publication/2004/OFR04_38/chapt_02.pdf

Cheema, M. R., Raza, S. M., & Ahmad, H. (1977). Stratigraphy of Pakistan. *Memoirs of the Geological Survey of Pakistan*, *12*, 138.

Chilingar, G. V., Bissell, H. J., & Fairbridge, R. W. (2011). *Carbonate rocks*. Elsevier.

Croizé, D., Bjørlykke, K., Jahren, J. and Renard, F., 2010. Experimental mechanical and chemical compaction of carbonate sand. Journal of Geophysical Research: Solid Earth, 115(B11).

Davies, G.R. (1970) Carbonate bank sedimentation, eastern Shark Bay, Western Australia. Am. Assoc. Petrol. Geol. Mem. v.13, p 85–168

Deghirmandjian O (2001) Identification and characterization of hydraulic flow units in the San Juan Formation, Orocual Field, Venezuela, Texas A&M University

Ding, L., Qasim, M., Jadoon, I.A.K., Khan, M.A., Xu, Q., Cai, F., Wang, H., Baral, U., Yue, Y., 2016. The India–Asia collision in north Pakistan: insight from the U–Pb detrital zircon provenance of Cenozoic foreland basin. Earth Planet. Sci. Lett. 455, 49–61

Dunham RJ (1962) Classifcation of carbonate rocks according to depositional texture. Am Assoc Pet Geol Mem 1:108–121

Eichenseer, H., & Luterbacher, H. (1992). The marine Paleogene of the Tremp Region (NE Spain)-depositional sequences, facies history, biostratigraphy and controlling factors. *Facies*, *27*, 119-151.

Farah, A., & DeJong, K. A. (1979). *Geodynamics of Pakistan*. Geological Survey of Pakistan.

Farah, A., & DeJong, K. A. (1979). *Geodynamics of Pakistan*. Geological Survey of Pakistan.

Ferraretti D, Gamberoni G, Lamma E (2012) Unsupervised and supervised learning in cascade for petroleum geology. Expert Syst Appl 39(10):9504–9514

Flügel E (2004) Microfacies of carbonate rocks: analysis interpretation and application. Springer-Verlag, Berlin, p 976

Flügel E (2010) Microfacies of carbonate rocks, analysis, interpretation and application, 2nd edn. Springer, Heidelberg, p 976

Flügel, E., 2004. Microfacies of carbonate rocks, analysis, interpretation and application: Springer-Verlag, 976.

Fügel, E., 2010. Microfacies of Carbonate Rocks: Analysis, Interpretation and Application. Springer.

Geel, T. (2000). Recognition of stratigraphic sequences in carbonate platform and slope deposits: empirical models based on microfacies analysis of Palaeogene deposits in southeastern Spain. *Palaeogeography, palaeoclimatology, palaeoecology*, *155*(3-4), p 211-238.

Ghazi, S. (2014). MICROFACIES AND DEPOSITIONAL SETTING OF THE EARLY EOCENE CHOR GALI FORMATION, CENTRAL SALT RANGE, PAKISTAN. *Pakistan Journal of Science*, *66*(2).

Grabau, A. W. (1924). *Principles of stratigraphy*. AG Seiler.

Green, O.R., Searle, M.P., Corfield, R.I., Corfield, R.M., 2008. Cretaceous – Tertiary carbonate platform evolution and the age of India – Asia collision along the Ladakh Himalaya (NW India). Extended Abstracts 23rd Himalayan KarakoramTibet workshop. Himalayan Journal of Sciences 5 (7), 54.

Hearn C, Ebanks W Jr, Tye R, Ranganathan V (1984) Geological factors influencing reservoir performance of the Hartzog Draw Field, Wyoming. J Petrol Technol 36(08):1335–1344

Hunt, J. M. (1995). Petroleum geochemistry and geology (textbook). *Petroleum Geochemistry and Geology (Textbook).(2 nd Ed.), WH Freeman Company*.

Iqbal, M., & Helmcke, D. (2004). Geological interpretation of earthquakes data of Zindapir Anticlinorium, Sulaiman foldbelt, Pakistan. *Pakistan journal of Hydrocarbon Research*, *14*, 41-47.

Jacobson, S. R. (1991). Petroleum Source Rocks and Organic Facies: Chapter 1: Petroleum Generation and Migration.

Jadoon, I. A., Lawrence, R. D., & Lillie3, R. J. (1994). Seismic data, geometry, evolution, and shortening in the active Sulaiman fold-and-thrust belt of Pakistan, southwest of the Himalayas. *AAPG bulletin*, *78*(5), 758-774.

Jadoon, I.A.K., Khurshid, A., 1996. Gravity and tectonic model across the Sulaiman fold belt and the Chaman fault zone in western Pakistan and eastern Afghanistan. Tectonophysics 254 (1–2), 89–109.

Jadoon, I.A.K., Zaib, M.O., 2018. Tectonic map of Sulaiman fold belt: 1:500,000 scale. COMSATS University Islamabad (Abbottabad Campus), Pakistan.

Jin, Y., McNutt, M.K., Zhu, Y.s., 1996. Mapping the descent of Indian and Eurasian plates beneath the Tibetan Plateau from gravity anomalies. J. Geophys. Res.: Solid Earth 101 (B5), 11275–11290.

Kazmi, A.H., Rana, R.A., 1982. Tectonic Map of Pakistan 1: 2 000 000: Map Showing Structural Features and Tectonic Stages in Pakistan. Geological Survey of Pakistan.

Lapponi, F., Bechstaedt, T., Boni, M., Banks, D. A., & Schneider, J. (2014). Hydrothermal dolomitization in a complex geodynamic setting (Lower Palaeozoic, northern Spain). *Sedimentology*, *61*(2), 411-443.

Laubach, S.E., J.E. Olson, M. R. Gross, 2009, *Mechanical and fracture stratigraphy*: AAPG Bulletin, v. 93, no. 11.

Lawrence, R. D., Yeats, R. S., Khan, S. H., Farah, A., & DeJong, K. A. (1981). Thrust and strike slip fault interaction along the Chaman transform zone, Pakistan. *Geological Society, London, Special Publications*, *9*(1), 363-370.

Lloyd, R.M., 1977. Porosity Reduction By Chemical Compaction-Stable-Isotope Model.

Lucia, F. J., Kerans, C., & Jennings, J. W. (2003). Carbonate reservoir characterization. *Journal of Petroleum Technology*, *55*(06), 70-72.

Malkani, M. S. (2010). Updated stratigraphy and mineral potential of Sulaiman Basin, Pakistan. *Sindh University Research Journal-SURJ (Science Series)*, *42*(2).

Malkani, M. S., & Mahmood, Z. (2017). Stratigraphy of Pakistan. Geological Survey of Pakistan, Memoir, 24, 1-134.

MATEU-VICENS, G. U. I. L. L. E. M., Pomar, L., & FERRÀNDEZ-CAÑADELL, C. A. R. L. E. S. (2012). Nummulitic banks in the upper Lutetian 'Buil level', Ainsa Basin, South Central Pyrenean Zone: the impact of internal waves. *Sedimentology*, *59*(2), 527-552.

Mirza, K., Akhter, N., Ejaz, A., & Zaidi, S. F. A. (2022). Biostratigraphy, microfacies and sequence stratigraphic analysis of the Chorgali Formation, Central Salt Range, northern Pakistan. *Solid Earth Sciences*, *7*(2), p 104-125.

Mode AW, Anyiam O, Onwuchekwa CN (2014) Flow unit characterization: key to delineating reservoir performance in "Aqua-field", Niger Delta, Nigeria. J Geol Soc India 84:701–708

Moqbel A, Wang Y (2011) Carbonate reservoir characterization with lithofacies clustering and porosity prediction. J Geophys Eng 8:592–598

Nebelsick, J. H., Rasser, M. W., & Bassi, D. (2005). Facies dynamics in Eocene to Oligocene circumalpine carbonates. *Facies*, *51*, 197-217.

Nichols, G., 2009. Sedimentology and stratigraphy. John Wiley & Sons.

Perez HH, Datta-Gupta A, Mishra S (2005) The role of electrofacies, lithofacies, and hydraulic flow units in permeability predictions from well logs: a comparative analysis using classification trees. SPE Reserv Eval Eng 8(2):143–155

Peters, K. E., & Cassa, M. R. (1994). Applied source rock geochemistry: Chapter 5: Part II. Essential elements.

Peters, K. E., & Cassa, M. R. (1994). Applied source rock geochemistry: Chapter 5: Part II. Essential elements.

Plastino A, Gonçalves EC, da Silva PN, Carneiro G, Azeredo RBV (2017) Combining classification and regression for improving permeability estimations from H NMR relaxation data. J Appl Geophys 146:5–102

Pomar, L., Baceta, J. I., Hallock, P., Mateu-Vicens, G., & Basso, D. (2017). Reef building and carbonate production modes in the west-central Tethys during the Cenozoic. *Marine and Petroleum Geology*, *83*, 261-304.

Prevot, R., Hatzfeld, D., Roecker, S. W., & Molnar, P. (1980). Shallow earthquakes and active tectonics in eastern Afghanistan. *Journal of Geophysical Research: Solid Earth*, *85*(B3), 1347-1357.

Qasim, M., Ding, L., Khan, M.A., Umar, M., Jadoon, I.A.K., Haneef, M., Baral, U., Cai, F., Shah, A., Yao, W., 2018. Late neoproterozoic–early palaeozoic stratigraphic succession, western Himalaya, north Pakistan: detrital zircon provenance and tectonic implications. Geol. J. 53 (5), 2258–2279.

Qayyum, M., Niem, A.R., Lawrence, R.D., 1996. Newly discovered Paleogene deltaic sequence in Katawaz basin, Pakistan, and its tectonic implications. Geology 24 (9), 835–838.

Quittmeyer, R. C., & Jacob, K. H. (1979). Historical and modern seismicity of Pakistan, Afghanistan, northwestern India, and southeastern Iran. *Bulletin of the Seismological Society of America*, *69*(3), 773-823.

Quittmeyer, R. C., & Jacob, K. H. (1979). Historical and modern seismicity of Pakistan, Afghanistan, northwestern India, and southeastern Iran. *Bulletin of the Seismological Society of America*, *69*(3), 773-823.

Rahim K, Reza R, Reza MH, Ali KI (2013) Analysis of the reservoir electrofacies in the framework of hydraulic flow units in the Whicher Range Field Perth Basin Western Australia. J Petrol Sci Eng 111:106–120

Reid, R.P. and Macintyre, I.G., 2000. Microboring versus recrystallization: further insight into the micritization process. Journal of Sedimentary Research, 70(1), pp.24- 28.

Reynolds, K., Copley, A., Hussain, E., 2015. Evolution and dynamics of a fold-thrust belt: the Sulaiman Range of Pakistan. Geophys. J. Int. 201 (2), 683–710.

Reynolds, K., Copley, A., Hussain, E., 2015. Evolution and dynamics of a fold-thrust belt: the Sulaiman Range of Pakistan. Geophys. J. Int. 201 (2), 683–710.

Roozpeykar, A., & Moghaddam, I. M. (2016). Benthic foraminifera as biostratigraphical and paleoecological indicators: an example from Oligo-Miocene deposits in the SW of Zagros basin, Iran. *Geoscience Frontiers*, *7*(1), 125-140.

Rowlands, D. (1978). The structure and seismicity of a portion of the southern Sulaiman Range, Pakistan. *Tectonophysics*, *51*(1-2), 41-56.

Sallam, E., Issawi, B., & Osman, R. (2015). Stratigraphy, facies, and depositional environments of the Paleogene sediments in Cairo–Suez district, Egypt. *Arabian Journal of Geosciences*, *8*, 1939-1964.

Sarkar, S. (2015). T hanetian–I lerdian coralline algae and benthic foraminifera from northeast I ndia: microfacies analysis and new insights into the T ethyan perspective. *Lethaia*, *48*(1), 13-28.

Selley, R. C., Cocks, L. R. M., & Plimer, I. R. (2005). *Encyclopedia of geology*. Elsevier Academic.

Serra O, Abbott HT (1980) The contribution of logging data to sedimentology and stratigraphic. In: SPE (Society of Petroleum Engineering) 9270, 55th annual fall technical conference and exhibition, Dallas, Texas

Serra-Kiel, J., Hottinger, L., Caus, E., Drobne, K., Ferrandez, C., Jauhri, A. K., ... & Zakrevskaya, E. (1998). Larger foraminiferal biostratigraphy of the Tethyan Paleocene and Eocene. *Bulletin de la Société géologique de France*, *169*(2), 281-299.

Serra-Kiel, J., i Herrero, A. T., i Palós, E. M., Briansó, E. S., i Cañadell, C. F., i Angrill, J. T., & i Masip, J. V. (2003). Marine and Transitional Middle/Upper Eocene Units of the Southeastern Pyrenean Forelan Basin (NE spain). Geologica Acta, 1(2), 177–177.

Shinn, E.A. and Robbin, D.M., 1983. Mechanical and chemical compaction in finegrained shallow-water limestones. Journal of Sedimentary Research, 53(2), pp.595-618.

Skalinski M, Kenter J (2013) Carbonate petrophysical rock typing—integrating geological attributes and petrophysical properties while linking with dynamic behavior. In: SPWLA 54th annual logging symposium, 22–26 June, New Orleans, Louisiana, Paper SPWLA-2013-A

Smith, G. L., & Simo, J. A. (1997). Carbonate diagenesis and dolomitization of the lower Ordovician Prairie du Chien Group. *Geoscience Wisconsin*, *16*, 1-16.

Stein, S., & Sella, G. F. (2002). Plate boundary zones: concept and approaches. In *Plate boundary zones* (Vol. 30, pp. 1-26). Washington, DC: AGU.

Szeliga, W., Bilham, R., Kakar, D. M., & Lodi, S. H. (2012). Interseismic strain accumulation along the western boundary of the Indian subcontinent. *Journal of Geophysical Research: Solid Earth*, *117*(B8).

Tahirkheli, R.K., 1979. The India-Eurasia Suture Zone in Northern Pakistan: Synthesis and Interpretation of Recent Data at Plate Scale: Geodynamics of Pakistan, pp. 125–130.

Tucker, D., Hildreth, W., Ullrich, T. and Friedman, R., 2007. Geology and complex collapse mechanisms of the 3.72 Ma Hannegan caldera, North Cascades, Washington, USA. Geological Society of America Bulletin, 119(3-4), pp.329-342.

Tucker, M. E. (Ed.). (2001). *Sedimentary petrology: an introduction to the origin of sedimentary rocks*. John Wiley & Sons. p 262.

Ullah, R., Fengjuin, N., Chengyong, Z., Izhar, S., Safdar, I., Xin, Z., & Ali, A. (2020). Occurrence of a likely tuff bed between the middle and upper Siwaliks, Taunsa area, Dera Ghazi Khan, eastern Sulaiman range, Pakistan. *International Journal of Economic and Environmental Geology*, *11*(1), 24-34.

Vernant, P., Nilforoushan, F., Hatzfeld, D., Abbassi, M. R., Vigny, C., Masson, F., ... & Chéry, J. (2004). Present-day crustal deformation and plate kinematics in the Middle East constrained by GPS measurements in Iran and northern Oman. *Geophysical Journal International*, *157*(1), 381-398.

Wanas, H. A. (2008). Cenomanian rocks in the Sinai Peninsula, Northeast Egypt: Facies analysis and sequence stratigraphy. *Journal of African Earth Sciences*, *52*(4-5), 125-138.

Waples, D. W., Kamata, H., & Suizu, M. (1992). The art of maturity modeling, part 1: finding a satisfactory geologic model. *AAPG bulletin*, *76*(1), 31-46.

Warraich, M. Y., Ogasawara, K., & Nishi, H. (2000). Late Paleocene to early Eocene planktic foraminiferal biostratigraphy of the Dungan Formation, Sulaiman Range, central Pakistan. *Paleontological Research*, *4*(4), 275-301.

Warwick, P. D., Johnson, E. A., & Khan, I. H. (1998). Collision-induced tectonism along the northwestern margin of the Indian subcontinent as recorded in the Upper Paleocene to Middle Eocene strata of central Pakistan (Kirthar and Sulaiman Ranges). *Palaeogeography, Palaeoclimatology, Palaeoecology*, *142*(3-4), 201-216.

Welte, D. H., & Tissot, P. (1984). *Petroleum formation and occurrence*. Springer-verlag.

Weyl, P.K., 1960. Porosity through dolomitization--Conservation-of-mass requirements. Journal of Sedimentary Research, 30(1), pp.85-90.

Wilson, J.L., 1975. Carbonate Facies in Geologic History. Springer Science & Business Media. P 471.

Yasin, Q., Du, Q., Ismail, A., & Shaikh, A. (2019). A new integrated workflow for improving permeability estimation in a highly heterogeneous reservoir of Sawan Gas Field from

well logs data. *Geomechanics and Geophysics for Geo-Energy and Geo-Resources*, 5(2), 121-142.